Electronic Supplementary Material (ESI) for Dalton Transactions.
This journal is © The Royal Society of Chemistry 2020

ELECTRONIC SUPPORTING INFORMATION

Role of aromatic vs aliphatic amine for variation of structural, electrical and catalytic behaviors in a series of silver phosphonate extended hybrid solids

Tanmay Rom and Avijit Kumar Paul*

Department of Chemistry, National Institute of Technology Kurukshetra, Kurukshetra-136119, Haryana, India.

E-mail: apaul@nitkkr.ac.in

Table of Contents:

Table S1. Selected bond distances and bond angles marked in compound **1**.

Bond	**Length (Å)**	**Bond**	**Angle (deg.)**
Ag(1)-N(1)	2.226(5)	N(1)-Ag(1)-N(1)#1	135.8(3)
Ag(1)-O(1)	2.613(4)	N(1)-Ag(1)-O(1)	88.4(6)
P(1)-O(1)	1.530(5)	O(1)-Ag(1)-O(1)#1	78.4(3)
P(1)-O(2)	1.556(5)	O(1)-Ag(1)-N(1)#1	127.5(5)
P(1)-O(3)	1.501(4)	O(3)-P(1)-O(1)	114.4(3)
		O(3)-P(1)-O(2)	112.0(3)
		O(1)-P(1)-O(2)	108.2(3)
Symmetry transformations used to generate equivalent atoms: #1; 0.5-x, y, 1.5-z			

Table S2. Selected bond distances and bond angles marked in compound **2**.

Bond	**Length (Å)**	**Bond**	**Length (Å)**
Ag(1)-N(2)	2.188(5)	P(1)-O(5)	1.493(5)
Ag(1)-O(7)#1	2.265(5)	P(1)-O(6)	1.519(5)
Ag(1)-O(4)	2.708(5)	P(1)-O(7)	1.594(5)
Ag(1)-O(6)	2.662(5)	P(2)-O(1)	1.521(5)
Ag(2)-N(1)	2.192(6)	P(2)-O(2)	1.484(5)
Ag(2)-O(1)	2.290(5)	P(2)-O(3)	1.585(5)
Ag(2)-O(7)#2	2.398(5)	**Ag(1)-Ag(2)#1**	3.1786(8)
Bond	**Angle (deg.)**	**Bond**	**Angle (deg.)**
N(2)-Ag(1)-O(7)#1	167.4(2)	O(1)-Ag(2)-O(7)#2	99.9(1)
O(6)-Ag(1)-O(4)#1	158.3(1)	Ag(1)-O(7)-Ag(2)#4	124.1(2)
O(6)-Ag(1)-O(7)#2	86.2(1)	O(5)-P(1)-O(7)	116.2(3)
O(6)-Ag(1)-N(2)#2	96.3(1)	O(5)-P(1)-O(6)	111.7(3)
O(4)-Ag(1)-N(2)#2	99.5(1)	O(7)-P(1)-O(6)	105.9(3)
O(4)-Ag(1)-O(7)#2	75.1(1)	O(2)-P(2)-O(1)	117.0(3)
N(1)-Ag(2)-O(1)	138.6(2)	O(2)-P(2)-O(3)	107.4(3)
N(1)-Ag(2)-O(7)#2	120.3(1)	O(1)-P(2)-O(3)	108.8(3)
Symmetry transformations used to generate equivalent atoms: #1; 1+x, 1-y, 0.5+z; #2; x, 1-y, -0.5+z; #4; x, 1-y, 0.5+z			

Table S3. Selected bond distances and bond angles marked in compound **3**.

Bond	**Length (Å)**	**Bond**	**Length (Å)**
Ag(1)-O(1)	2.275(3)	**Ag(2)-Ag(2)#4**	**3.1495(9)**
Ag(1)-O(3)#1	2.403(3)	**Ag(2)-Ag(2)#5**	**3.1927(8)**
Ag(1)-O(2)#2	2.443(4)	P(1)-O(1)	1.518(4)
Ag(1)-O(6)#3	2.505(4)	P(1)-O(2)	1.523(4)
Ag(1)-O(6)	2.601(3)	P(1)-O(3)	1.544(4)
Ag(2)-O(1)	2.309(4)	P(2)-O(5)	1.552(4)
Ag(2)-O(2)#4	2.383(4)	P(2)-O(6)	1.529(4)
Ag(2)-O(2)#1	2.461(4)	P(2)-O(7)	1.511(4)
Ag(2)-O(5)#4	2.486(4)		
Bond	**Angle (deg.)**	**Bond**	**Angle (deg.)**
O(1)-Ag(1)-O(3)#1	104.72(13)	O(2)#1-Ag(2)-O(5)#4	86.72(12)
O(1)-Ag(1)-O(2)#2	130.34(13)	Ag(1)-O(1)-Ag(2)	108.94(14)
O(3)#1-Ag(1)-O(2)	97.67(12)	Ag(2)#4-O(1)-Ag(1)#2	90.80(12)
O(1)-Ag(1)-O(6)#3	126.93(13)	Ag(2)#4-O(1)-Ag(2)#6	82.44(11)
O(3)#1-Ag(1)-O(6)#3	97.97(12)	Ag(1)#2-O(1)-Ag(2)#6	117.00(14)
O(2)#2-Ag(1)-O(6)#3	91.98(12)	O(1)-P(1)-O(2)	112.6(2)
O(1)-Ag(2)-O(2)#4	164.73(13)	O(1)-P(1)-O(3)	111.9(2)
O(1)-Ag(2)-O(2)#1	97.71(12)	O(2)-P(1)-O(3)	110.3(2)
O(2)#4-Ag(2)-O(2)#1	97.56(11)	O(7)-P(2)-O(6)	112.7(2)
O(1)-Ag(2)-O(5)#4	101.89(14)	O(7)-P(2)-O(5)	111.5(2)
O(2)#4-Ag(2)-O(5)#4	78.61(12)	O(6)-P(2)-O(5)	110.5(2)
Symmetry transformations used to generate equivalent atoms: #1: -1+x, y, z; #2: 1-x, 2-y, 2-z; #3: x, 1+y, z; #4: 1-x, 1-y, 2-z; #5: -x, 1-y, 2-z; #6: 1+x, y, z.			

Table S4. Selected bond distances and bond angles marked in compound **4**.

Bond	**Length (Å)**	**Bond**	**Length (Å)**
Ag(1)-O(1)	2.295(6)	**Ag(1)-Ag(4)**	**3.3041(9)**
Ag(1)-O(2)#2	2.380(5)	**Ag(2)-Ag(3)#4**	**3.1421(9)**
Ag(1)-O(3)#1	2.349(5)	**Ag(2)-Ag(5)**	**3.1671(10)**
Ag(1)-O(12)#2	2.409(6)	**Ag(2)-Ag(5)#4**	**3.1816(9)**
Ag(2)-O(2)	2.370(6)	**Ag(3)-Ag(2)#5**	**3.1421(9)**
Ag(2)-O(4)	2.412(5)	**Ag(3)-Ag(5)#5**	**3.0683(10)**
Ag(2)-O(5)#4	2.415(6)	**Ag(4)-Ag(1)#4**	**3.0549(9)**
Ag(2)-O(8)	2.384(5)	**Ag(4)-Ag(1)#2**	**3.1922(9)**
Ag(2)-O(12)	2.633(5)	**Ag(5)-Ag(2)#3**	**3.1816(9)**
Ag(3)-O(4)	2.287(6)	**Ag(5)-Ag(3)#5**	**3.0683(10)**
Ag(3)-O(6)#4	2.405(5)	P(1)-O(1)	1.519(6)
Ag(3)-O(9)#5	2.450(6)	P(1)-O(2)	1.535(5)
Ag(4)-O(1)	2.328(6)	P(1)-O(3)	1.531(5)
Ag(4)-O(3)#2	2.348(5)	P(2)-O(4)	1.514(6)
Ag(4)-O(11)#2	2.405(6)	P(2)-O(5)	1.503(6)
Ag(4)-O(15)	2.396(6)	P(2)-O(6)	1.559(5)
Ag(5)-O(3)	2.594(6)	P(3)-O(8)	1.548(5)
Ag(5)-O(5)	2.444(6)	P(3)-O(9)	1.515(6)
Ag(5)-O(9)	2.502(6)	P(3)-O(10)	1.503(6)
Ag(5)-O(11)	2.360(6)	P(4)-O(11)	1.510(6)
Ag(5)-O(12)#3	2.467(6)	P(4)-O(12)	1.507(6)
Ag(1)-Ag(1)#1	**3.0051(12)**	P(4)-O(13)	1.589(5)
Ag(1)-Ag(4)#2	**3.1922(9)**	**Ag(1)-Ag(4)#3**	**3.0549(9)**

Bond	Angle (deg.)	Bond	Angle (deg.)
O(1)-Ag(1)-O(3)#1	144.48(18)	O(12)#3-Ag(5)-O(3)	75.97(18)
O(1)-Ag(1)-O(2)#2	117.86(19)	O(9)-Ag(5)-O(3)	149.68(18)
O(3)#1-Ag(1)-O(2)#2	97.63(18)	Ag(1)-O(1)-Ag(4)	91.24(18)
O(1)-Ag(1)-O(12)#2	97.6(2)	Ag(2)-O(2)-Ag(1)#2	92.24(19)
O(3)#1-Ag(1)-O(12)#2	81.8(2)	Ag(4)-O(3)-Ag(1)#1	81.15(16)
O(2)#2-Ag(1)-O(12)#2	91.8(2)	Ag(4)-O(3)-Ag(5)	89.87(17)
O(2)-Ag(2)-O(8)	161.95(18)	Ag(1)#1-O(3)-Ag(5)	99.66(19)
O(2)-Ag(2)-O(4)	83.66(19)	Ag(3)-O(4)-Ag(2)	100.5(2)
O(8)-Ag(2)-O(4)	114.19(19)	Ag(2)#3-O(5)-Ag(5)	81.80(17)
O(4)-Ag(3)-O(6)#4	115.63(19)	Ag(3)#5-O(9)-Ag(5)	76.57(16)
O(4)-Ag(3)-O(9)#5	122.09(19)	Ag(5)-O(11)-Ag(4)#2	94.4(2)
O(1)-Ag(4)-O(3)#2	120.63(19)	Ag(1)#2-O(12)-Ag(5)#4	101.7(2)
O(1)-Ag(4)-O(15)	106.9(2)	O(1)-P(1)-O(3)	112.1(3)
O(1)-Ag(4)-O(11)#2	107.4(2)	O(1)-P(1)-O(2)	111.6(3)
O(3)#2-Ag(4)-O(15)	129.71(19)	O(3)-P(1)-O(2)	113.1(3)
O(3)#2-Ag(4)-O(15)#2	87.63(19)	O(5)-P(2)-O(4)	113.1(3)
O(15)-Ag(4)-O(11)#2	93.4(2)	O(5)-P(2)-O(6)	110.0(3)
O(11)-Ag(5)-O(5)	153.9(2)	O(4)-P(2)-O(6)	110.8(3)
O(11)-Ag(5)-O(12)#3	89.2(2)	O(10)-P(3)-O(9)	112.3(3)
O(5)-Ag(5)-O(12)#3	99.8(2)	O(10)-P(3)-O(8)	111.7(3)
O(11)-Ag(5)-O(9)	81.91(19)	O(9)-P(3)-O(8)	111.4(3)
O(5)-Ag(5)-O(9)	109.53(19)	O(12)-P(4)-O(11)	118.1(4)
O(12)#3-Ag(5)-O(9)	129.83(19)	O(12)-P(4)-O(13)	107.3(3)
O(11)-Ag(5)-O(3)	83.10(19)	O(11)-P(4)-O(13)	108.6(3)
O(5)-Ag(5)-O(3)	75.55(17)		

Symmetry transformations used to generate equivalent atoms: #1: 2-x, 1-y, 2-z; #2: 1-x, 1-y, 2-z; #3: 1+x, y, z; #4: -1+x, y, z; #5: 1-x, 1-y, 1-z.

Table S5: Selected hydrogen-bond distances (Å) and angles (°) for compound **1**.

Sl. No.	Donor --- H....Acceptor	D – H (A˚)	H... A (A˚)	D.... A (A˚)	D -- H.... A (°)
1	O2---H2A...O3$^{\#1}$	0.89(9)	1.68(9)	2.563(7)	168(10)
3	C1---H1...O2	0.93	2.60	3.376(9)	142
4	C2---H2...O3$^{\#2}$	0.93	2.55	3.456(9)	165
#1: -x,1-y,1-z; #2: 1-x,1-y,1-z					

Table S6: Selected hydrogen-bond distances (Å) and angles (°) for compound **2**.

Sl. No.	Donor --- H....Acceptor	D – H (A˚)	H... A (A˚)	D.... A (A˚)	D -- H.... A (°)
1	O4---H4...O3	0.82	2.59	2.991(8)	123
2	O4---H4...O101	0.82	2.13	2.714(9)	128
3	O101---H10A...O5$^{\#3}$	0.85(13)	2.03(14)	2.813(9)	152(16)
4	O101---H10B...O2$^{\#4}$	0.85(5)	1.90(7)	2.726(9)	166(8)
5	O100---H10C...O2$^{\#3}$	0.85(7)	2.01(10)	2.700(9)	138(10)
6	O100---H10E...O101	0.85(9)	2.60(9)	3.148(10)	124(7)
7	O100---H10E...O5$^{\#3}$	0.85(9)	2.01(9)	2.830(9)	163(8)
8	C5---H5...O5$^{\#1}$	0.93	2.39	3.266(9)	158
9	C8---H8...O100$^{\#2}$	0.93	2.53	3.410(10)	159
10	C9---H9...O4	0.93	2.53	3.169(9)	126
.#1: -1+x,-y,-1/2+z; #2: x,-y,1/2+z; #3: -1/2+x,1/2-y,-1/2+z; #4: -1/2+x,1/2-y,1/2+z					

Table S7: Selected hydrogen-bond distances (Å) and angles (°) for compound **3**.

Sl. No.	Donor --- H....Acceptor	D – H (A˚)	H... A (A˚)	D.... A (A˚)	D -- H.... A (°)
1	N1---H1A...O7	0.90	2.73	3.308(6)	122
2	N1---H1B...O4$^{\#2}$	0.90	2.56	3.204(7)	129
3	O4---H4...O6$^{\#1}$	0.82	2.16	2.907(5)	151
4	C3---H3B...O4$^{\#1}$	0.97	2.55	3.436(7)	152
5	C4---H4A...O7$^{\#2}$	0.97	1.72	2.688(6)	172
6	C4---H4B...O6$^{\#3}$	0.97	1.92	2.884(5)	176
7	C4---H4B...O7$^{\#3}$	0.97	2.56	3.105(6)	116
#1: -1+x,y,z; #2: -x,1-y,1-z; #3: 1-x,1-y,1-z					

Table S8: Selected hydrogen-bond distances (Å) and angles (°) for compound **4**.

Sl. No.	Donor --- H....Acceptor	D – H (A˚)	H... A (A˚)	D.... A (A˚)	D -- H.... A (°)
1	N1---H1A...O10$^{\#5}$	0.90	2.57	3.293(11)	138
2	N1---H1B...O7	0.90	2.67	3.30(8)	120
3	O7---H7...O2$^{\#1}$	0.82	2.30	2.910(8)	131
4	O14---H14...O10	0.82	2.59	3.026(8)	115
5	O15---H15...O13$^{\#4}$	0.82	2.12	2.878(8)	153
6	O15---H16...O7$^{\#4}$	0.86(6)	1.93(6)	2.783(8)	175
7	C5---H5A...O10$^{\#3}$	0.97	1.67	2.616(9)	164
8	C5---H5B...O9$^{\#2}$	0.97	1.93	2.852(9)	157
9	C5---H5B...O10$^{\#2}$	0.97	2.55	3.320(9)	136
10	C6---H6A...O10$^{\#2}$	0.97	2.38	3.198(10)	142
#1: -1+x,y,z; #2: -1+x,y,1+z; #3: x,y,1+z; #4: 1+x,y,z; #5:1-x,-y,-z					

Table S9: Optimized conditions for the cyanosilylation reaction of aromatic aldehyde with compounds **1** – **4** as catalyst.

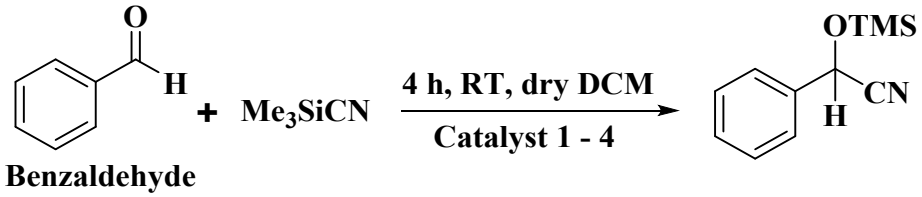

Benzaldehyde

Catalyst	Temperature (˚C)	Time (h)	Isolated yield (%)	TON
1	**RT**	**4**	**90**	**4.50**
2			**99**	**4.95**
3			**84**	**4.20**
4			**96**	**4.80**
1	RT	2	64	3.20
2			75	3.75
3			58	2.90
4			69	3.45
1	RT	6	91	4.55
2			99	4.95
3			85	4.25
4			95	4.75
1	0-5	4	78	3.90
2			86	4.30
3			71	3.55
4			82	4.10
$AgNO_3$	RT	4	35	1.75
4,4′-bipyridine	RT	4	25	1.25
Piperazine	RT	4	11	0.55
HEDP	RT	4	<10	<0.50
No catalyst	RT	4	<5	<0.25

Reaction conditions: Benzaldehyde (0.5 mmol), Me_3SiCN (0.75 mmol), catalyst (0.1 mmol), and dry DCM (10 mL), room temperature, 4h. TON = %conversion (mmol of substrate/mmol of catalyst).

Table S10: Optimized conditions for the cyanosilylation reaction of imines with compounds **1 – 4** as catalyst.

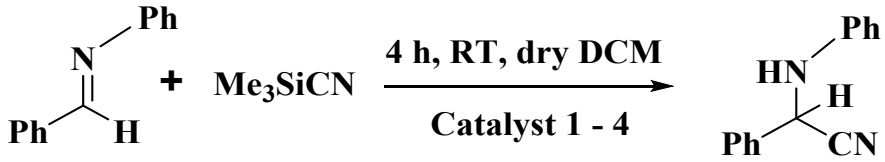

N-benzilidine aniline

Catalyst	Temperature (˚C)	Time (h)	Isolated yield (%)	TON
1	**RT**	**4**	**88**	**4.40**
2			**98**	**4.90**
3			**82**	**4.10**
4			**93**	**4.65**
1	RT	2	69	3.45
2			72	3.60
3			62	3.10
4			67	3.35
1	RT	6	93	4.65
2			98	4.90
3			90	4.50
4			93	4.65
1	0-5	4	80	4.00
2			83	4.15
3			75	3.75
4			79	3.95
$AgNO_3$	RT	4	30	1.50
4,4′-bipyridine	RT	4	22	1.10
Piperazine	RT	4	12	0.60
HEDP	RT	4	<8	<0.40
No catalyst	RT	4	<5	<0.25

Reaction conditions: N-benzylideneaniline (0.5 mmol), Me_3SiCN (0.75 mmol), catalyst (0.1 mmol), and dry DCM (10 mL), room temperature, 4h. TON = %conversion (mmol of substrate/mmol of catalyst).

Table S11: Optimized condition for the cyclic ketal formation reactions employing for the catalysts **1** – **4.**

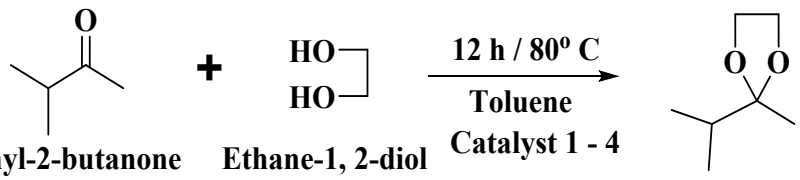

3-Methyl-2-butanone **Ethane-1, 2-diol**

Catalyst	Temperature (˚C)	Time (h)	Isolated yield (%)	TON
1	**80**	**12**	**91**	**291.2**
2			**96**	**307.2**
3			**80**	**256.0**
4			**88**	**281.6**
1	100	12	89	284.8
2			94	300.8
3			77	246.4
4			86	275.2
1	60	12	82	262.4
2			88	281.6
3			70	224.0
4			75	240.0
1	80	15	90	288.0
2			97	310.4
3			82	262.4
4			89	284.8
1	80	9	78	249.6
2			84	268.8
3			64	204.8
4			70	224.0
$AgNO_3$	80	12	32	102.4
4,4′-bipyridine	80	12	18	57.6
Piperazine	80	12	15	48.0
HEDP	80	12	<12	<38.4
No catalyst	80	12	<5	<16.0

Reaction conditions: 3-Methyl-2-butanonae (16 mmol), ethanol (16 mmol), catalyst (0.05 mmol) and toluene (10 mL), 80 ˚C, 12h. TON = %conversion (mmol of substrate/mmol of catalyst).

Table S12: Optimized condition for the ester formation reactions employing for the catalysts **1** – **4**.

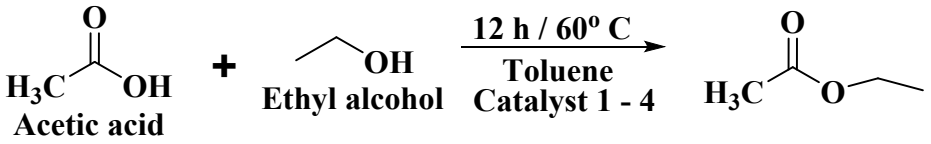

Catalyst	Temperature (˚C)	Time (h)	Isolated yield (%)	TON
1	**60**	**12**	**61**	**195.2**
2			**69**	**220.8**
3			**50**	**160.0**
4			**55**	**176.0**
1	80	12	55	176.0
2			62	198.4
3			47	150.4
4			50	160.0
1	40	12	49	156.8
2			55	176.0
3			45	144.0
4			48	153.6
1	60	15	62	198.4
2			68	217.6
3			50	160.0
4			56	179.2
1	60	9	54	172.8
2			62	198.4
3			42	134.4
4			48	153.6
$AgNO_3$	60	12	15	48.0
4,4′-bipyridine	60	12	<10	<32.0
Piperazine	60	12	<5	<16.0
HEDP	60	12	<10	<32.0
No catalyst	60	12	<5	<16.0

Reaction conditions: Acetic acid (16 mmol), ethanol (16 mmol), catalyst (0.05 mmol) and toluene (10 mL), 60 ˚C, 12h. TON = %conversion (mmol of substrate/mmol of catalyst).

Table S13. Comparison table of crystallographic parameters between various reported silver phosphonate frameworks and our present compounds.

Chemical Formula and Formula Weight (F.W.)	**Crystal System**	**Space Group**	**a (Å), b (Å), c (Å)**	**V (Å)**	**Z**	**D (g cm^{-3})**	**μ (min^{-1})**	**GOF on F^2**	**Ref. No.**
$Ag_4O_6P_2C_2H_4$ F.W. = 617.47	Monoclinic	$P2_1/n$	6.0115(16), 8.630(2,) 8.462(2)	435.1(2)	2	4.713	9.231	1.196	[S1]
$AgUO_2[CH_2(PO_3)(PO_3H)]$ F.W. = 549.87	Orthorhombic	*Pbca*	12.0098(7), 10.3144(6), 12.2260(7)	1514.48(15)	8	4.823	24.379	1.272	[S2]
$Ag_2UO_2[CH_2(PO_3)_2]$ F.W. = 657.74	Monoclinic	$P2_1/n$	7.9919(4), 12.5811(6), 8.1506(4)	814.63(7)	4	2.99	24.999	1.059	[S2]
$C_{14}H_{18}Ag_2N_2O_6P_2$ F.W = 587.98	Monoclinic	*P*2/*c*	11.7570(14), 4.6361(5), 16.3047(18)	866.75(17)	2	2.253	2.480	1.064	[S3]
$C_{35}H_{40}Ag_2N_4O_{10}P_3$ F.W. = 985.36	Triclinic	*P*-1	10.4999(7), 12.1860(8), 15.1329(9)	1827.5(2)	2	1.791	1.267	1.031	[S3]
$C_{12}H_{14}Ag_4O_8P_2$ F.W. = 779.48	Monoclinic	$P2_1/c$	8.246(1), 28.040(4), 8.126(1)	1859.3(4)	4	2.771	4.360	1.152	[S4]
$C_{14}H_{13}Ag_2NO_5P_2$ F.W. = 552.78	Triclinic	*P*-1	6.0537(9), 11.2351(2), 12.7177(1)	851.9(2)	2	2.156	2.510	1.017	[S4]
$C_{30}H_{21}Ag_{11}F_6O_{16}P_4$ F.W. = 2061.92	Monoclinic	*C*2/*c*	32.021(3), 13.148(1), 10.017(9)	4203.2(7)	4	3.258	5.252	1.101	[S5]
$Ag_4P_2O_6C_{12}H_{10}$ F.W. = 743.62	Monoclinic	$P2_1/c$	5.6657(3), 10.1483(5), 29.733(2)	1709.51(2)	4	2.89	−	0.927	[S6]
$AgC_6H_7P_2O_6$ F.W. = 343.9	Triclinic	*P*-1	5.7484(2), 7.7389(3), 20.8271(8)	919.77(2)	4	2.49	−	1.015	[S7]
$C_{150}H_{282}Ag_{45}O_{34}P_9S_{29}$ F.W. = 8692.57	Hexagonal	*P*-62*c*	20.6340(12), 20.6340(12), 36.384(4)	13416(2)	2	−	3.520	1.502	[S8]
$AgP_2O_8N_2C_{11}H_{10}$ F.W. = 468.02	Monoclinic	*P*2/*n*	5.4579(5), 10.4871(9), 13.0653(12)	747.31(12)	2	2.080	1.609	1.348	**Present work**
$Ag_2P_2O_9N_2C_{12}H_{16}$ F.W. = 609.95	Monoclinic	*Cc*	13.7091(4), 18.1676(5), 7.1474(2)	1776.12(9)	4	2.281	2.437	1.177	**Present work**
$Ag_2P_2O_7NC_4H_{10}$ F.W. = 461.81	Triclinic	*P*-1	5.6217(2), 6.9511(2), 13.1285(4)	498.72(3)	2	3.069	4.267	1.286	**Present work**

$Ag_5P_4O_{16}NC_6H_{16}$ F.W. = 1021.43	Triclinic	*P*-1	5.7341(3), 13.4208(8), 13.6754(8)	1019.08(10)	2	3.329	5.114	1.210	**Present work**

Table S14. Comparison table of average Ag–O and Ag−Ag bond distance (Å) values between reported silver phosphonate frameworks and our present compounds.

Chemical Formula	**Average Ag–O bond distance (Å)**	**Average Ag−Ag bond distance (Å)**	**Reference No.**
$Ag_4O_6P_2C_2H_4$	2.291	3.143	[S1]
$AgUO_2[CH_2(PO_3)(PO_3H)]$	2.507	–	[S2]
$Ag_2UO_2[CH_2(PO_3)_2]$	2.386	3.246	[S2]
$C_{14}H_{18}Ag_2N_2O_6P_2$	2.183	3.226	[S3]
$C_{35}H_{40}Ag_2N_4O_{10}P_3$	2.662	3.181	[S3]
$C_{12}H_{14}Ag_4O_8P_2$	2.372	3.151	[S4]
$C_{14}H_{13}Ag_2NO_5P_2$	2.381	3.056	[S4]
$C_{30}H_{21}Ag_{11}F_6O_{16}P_4$	–	3.075	[S5]
$Ag_4P_2O_6C_{12}H_{10}$	2.401	3.174	[S6]
$AgC_6H_7P_2O_6$	2.346	–	[S7]
$C_{150}H_{282}Ag_{45}O_{34}P_9S_{29}$	2.355	3.142	[S8]
$AgP_2O_8N_2C_{11}H_{10}$	**2.613**	–	**Present work**
$Ag_2P_2O_9N_2C_{12}H_{16}$	**2.464**	**3.178**	**Present work**
$Ag_2P_2O_7NC_4H_{10}$	**2.429**	**3.170**	**Present work**
$Ag_5P_4O_{16}NC_6H_{16}$	**2.422**	**3.154**	**Present work**

Table S15. Comparison table of room temperature dielectric permittivity values between different reported MOFs and our present compounds.

Entry	**Different Metal-organic frameworks**	**Dielectric permittivity (ε′) at room temperature for ν = 10^3 Hz**	**Reference**
1	$[(H_3betc)(H\text{-}Hopip)_{0.5}(H_2O)]$ (OCC 1) $[(H_3betc)_2(H_2\text{-}Mepip)(H_2O)]$ (OCC 2)	~135 ~500	[S9]
2	$[Cu_2(EBTC)(H_2O)2\cdot 8H_2O\cdot DMF\cdot DMSO]_n$ (EBTC = 1,10-ethynebenzene3,3′,5,5′-tetracarboxylate)	~35	[S10]
3	$[C_6Apy][PbI_3]$ (C_6-Apy+ = 1-hexyl-4-aminopyridinium)	~1000	[S11]
4	4-(4-(4nitrobenzylideneamino) benzyl) oxazolidin-2-one (NBOA) 4-(4-(4chlorobenzylideneamino) benzyl) oxa-zolidin-2-one (CBOA) 4-(4-(4-hydroxybenzylideneamino)benzyl) oxazolidin-2-one (HBOA)	~150 ~400 ~800	[S12]
5	$[Ag_2(CA)]_n$	~34	[S13]
6	$[Zn_3btc_2\{Cr_3O(isonic)_6(H_2O)_2(OH)\}]\cdot(DMF)_{15.5}(H_2O)_8$ (H3btc=1,3,5-benzenetricarboxylic acid; isonic = isonicotinicate)	~155	[S14]
7	FeF_3(2,2′-bpy)	~100	[S15]
8	Q[8]$(CuCl_2)_{0.75}$.30(H2O) (Q[8] = cucurbit[8]- uril)	~2000	[S16]
9	Cd(hpip)$Br_2]_n$ [hpip = homopiperazine]	~300	[S17]
10	**Compound 1** **Compound 2** **Compound 3** **Compound 4**	**157** **191** **3408** **5990**	**Present Work**

Table S16. Comparison of the catalytic activity with reported aromatic aldehyde and imines cyanosilylation reactions catalyzed by various catalysts.

Entry	Catalyst used for aromatic aldehyde cyanosilylation reactions	Temperature (°C) and Time	Yield (%)	Ref.
1	$[Ag_4(apym)_4(SiW_{12}O_{40})]_n$, where apym = 2-aminopyrimidine	RT, 4 h.	96.2	[S18]
2	Eu-POM Tb-POM Yb-POM	RT, 6 h. RT, 6 h. RT, 6 h.	76 70 71	[S19]
3	Al/Fe-ITQ-NO2 98 Al-ITQ-Br	RT, 5 h. RT, 5 h.	98 88	[S20]
4	BINAPDA-Zr-MOF	RT, 5 h.	95	[S21]
5	La-BTTc	RT, 2 h.	82	[S22]
6	[Cd(PBA)(DMF)]·DMF.	RT, 8 h.	89	[S23]
7	$[Eu_2(PDC)_3 \cdot 2H_2O] \cdot 4H_2O$	RT, 3 h.	93	[S24]
8	**Catalyst 1** **Catalyst 2** **Catalyst 3** **Catalyst 4**	RT, 4 h. RT, 4 h. RT, 4 h. RT, 4 h.	**90** **99** **84** **96**	**Present Work**
Entry	**Catalyst used for imines cyanosilylation reactions**	**Temperature (°C) and Time**	**Yield (%)**	**Ref.**
1	$\{[In_3(NIPH)_3(HNIPH)(OH)_2]\cdot 4H_2O\}_n$	RT, 24 h.	96	[S25]
2	$\{[Cu_{3(}hbpdc)(OH)_2(H_2O)]\cdot 2H_2O\}_n$ $\{[Cu_{2(}hbpdc)(H_2O)]\}_n$	RT, 4 h. RT, 4 h.	95 93	[S26]
3	$\{[Cd(4,4'bpy)_2(H_2O)_2](NO_3)_2\cdot 4H_2O\}_n$	0°C, 1 h.	97	[S27]
4	$[Cd_2(H_2O)(C_2H_2N_3)(SO_4)]$ $[Cd_5(OH)_2(CH_2N_5)_4(SO_4)_2]$ $[Cd_2(OH)(H_2O)(C_2H_3N_4)(SO_4)]\cdot 2H_2O$	0°C, 2 h. 0°C, 2 h. 0°C, 2 h.	98 98 98	[S28]
5	$[Ag_8(SO_4)_4(C_3H_6N_6)_3]$	0°C, 2 h.	99	[S29]
6	$[Cd(L)(H_2O)]\cdot H_2O$, CP - **I** [Cd(L)], CP - **II**	RT, 4 h. RT, 4 h.	81 70	[S30]
7	$[Cd(NH_3CH_2COO)(SO_4)]$	0°C, 2 h	98	[S31]
8	**Catalyst 1** **Catalyst 2** **Catalyst 3** **Catalyst 4**	RT, 4 h. RT, 4 h. RT, 4 h. RT, 4 h.	**88** **98** **82** **93**	**Present Work**

		RT, 4 h.		

Table S17. Comparison of the catalytic activity with reported cyclic ketal and ester formation reaction catalyzed by various catalysts.

Entry	**Catalyst**	**Temperature (°C) and Time**	**Yield of cyclic ketal formation (%)**	**Yield of ester formation (%)**	**Ref.**
1	$[Zn(S_2O_3)(C_{13}H_{14}N_2)]$, **I** $[Zn(S_2O_3)(C_{10}H_{10}N_2)]_2$, **II** $[Zn(S_2O_3)(C_{12}H_{10}N_2)].H_2O$, **III** $[Zn_3(S_2O_3)_3(C_{12}H_{12}N_2)_3].3H_2O$, **IV**	60, 12 h. 60, 12 h. 60, 12 h. 60, 12 h.	94 92 91 90	- - - -	[S32]
2	CuL-Br CuL-PF_6 2D-Ag	110, 12 h 110, 12 h 110, 12 h	67 93 63	- - -	[S33]
3	Ag_2(4,4′-bipy)$_2$($O_3SCH_2CH_2SO_3$).4H_2O (SLUG-21)	110, 12 h	97	57	[S34]
4	$[Ag_8 (SO_4)_4(C_3H_6N_6)_3]$, **I**	60, 10 h.	98	55	[S29]
6	**Catalyst 1** **Catalyst 2** **Catalyst 3** **Catalyst 4**	80 and 60,12 h. 80 and 60,12 h. 80 and 60,12 h. 80 and 60,12 h.	**91** **96** **80** **88**	**61** **69** **50** **55**	**Present Work**

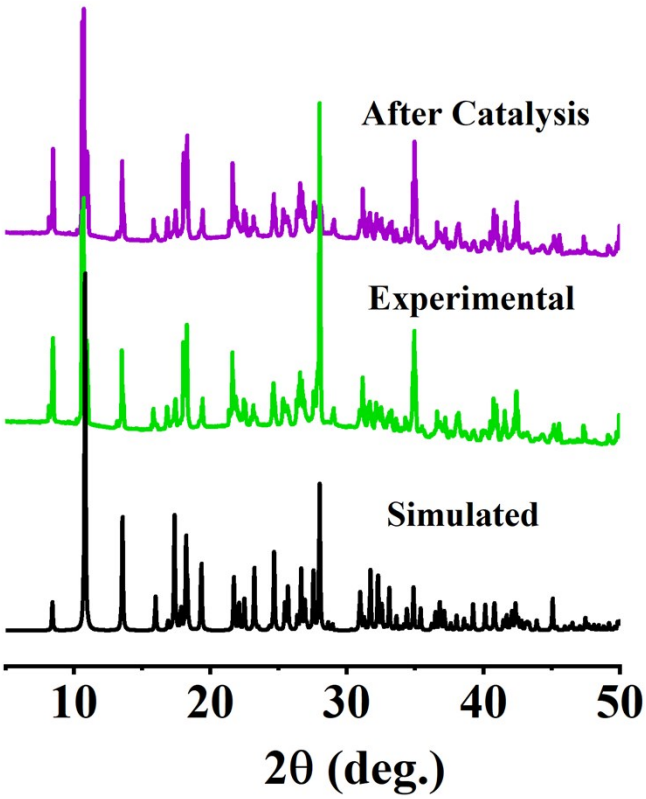

Figure S1: X-ray powder diffraction (Cu Kα) pattern of compound **1**; simulated (black), as-synthesized (light green), after catalysis (violet), respectively.

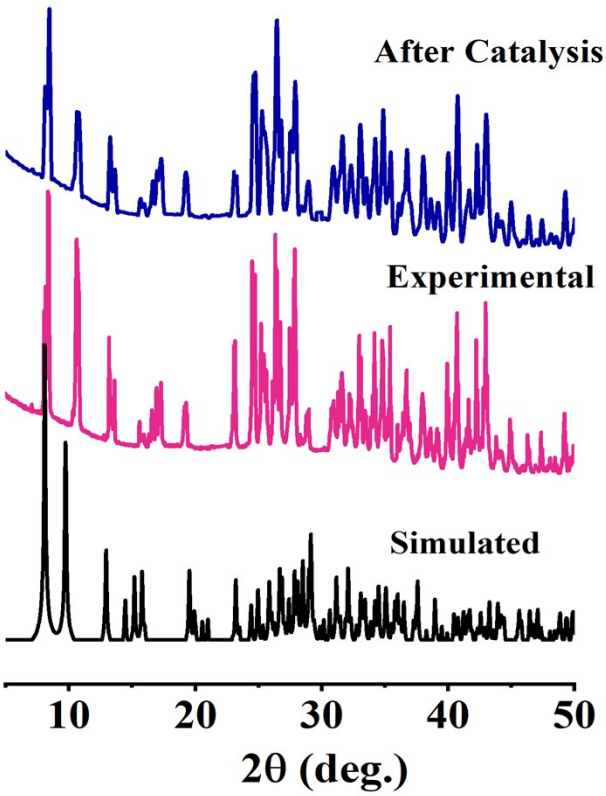

Figure S2: X-ray powder diffraction (Cu Kα) pattern of compound **2**; simulated (black), as-synthesized (pink), after catalysis (royal blue), respectively.

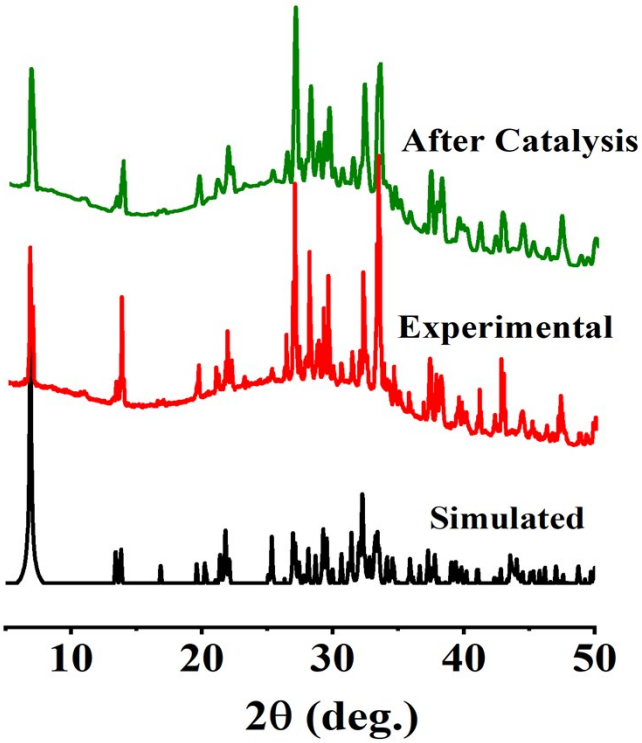

Figure S3: X-ray powder diffraction (Cu Kα) pattern of compound **3**; simulated (black), as-synthesized (red), after catalysis (green), respectively.

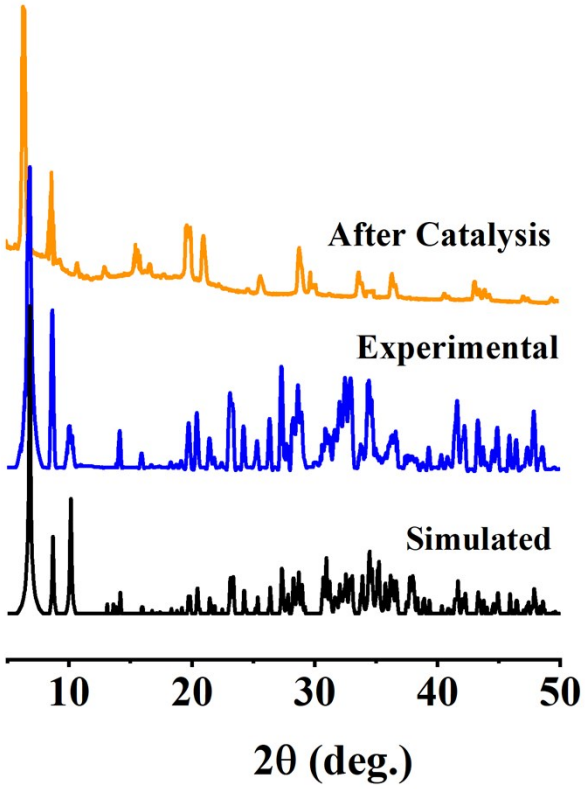

Figure S4: X-ray powder diffraction (Cu Kα) pattern of compound **4**; simulated (black), as-synthesized (blue), after catalysis (pink), respectively.

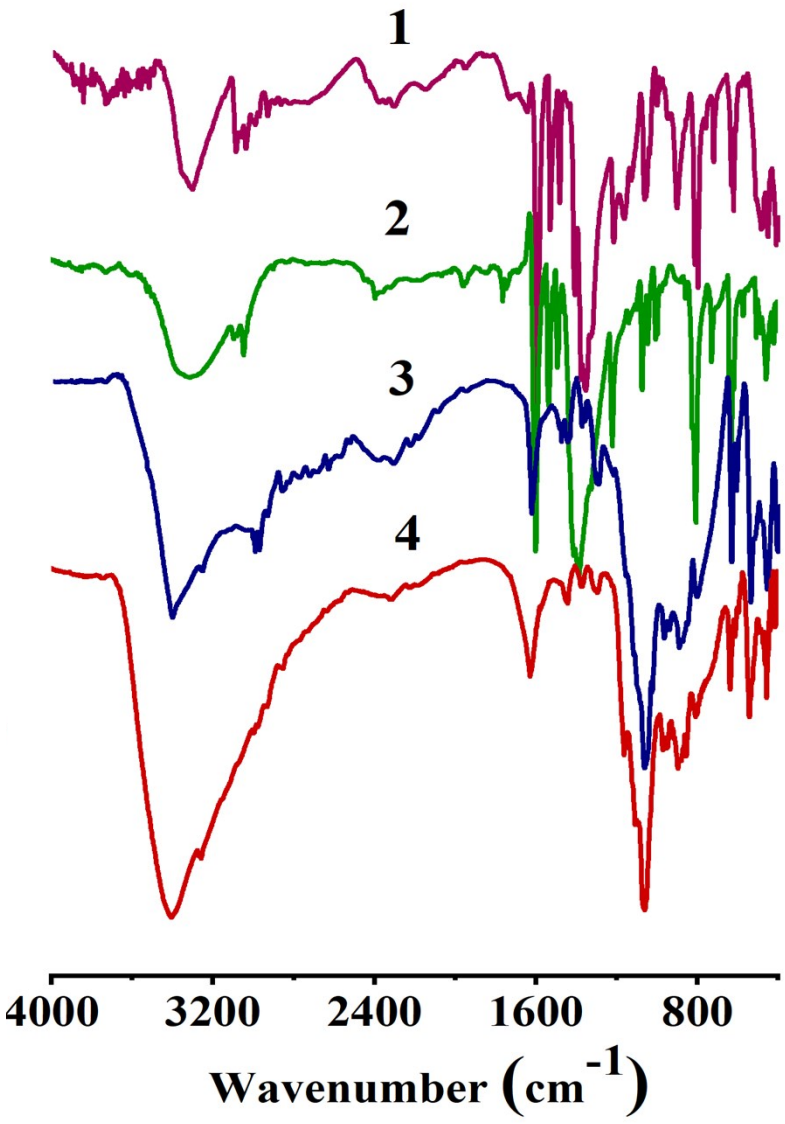

Figure S5: FT-IR spectra of compounds **1** – **4**.

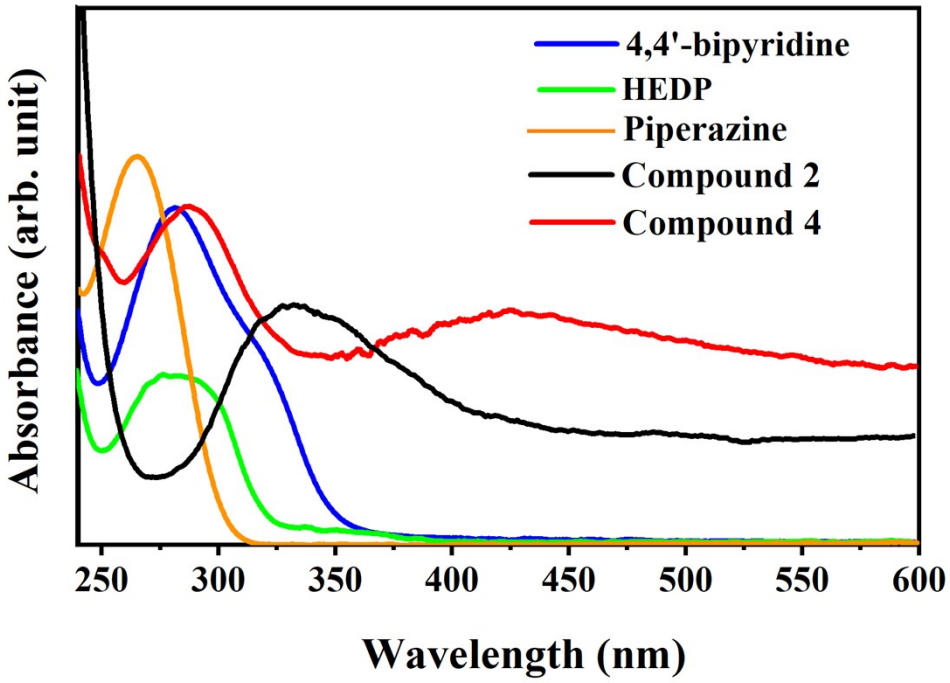

Figure S6: The UV-Visible absorption spectrum of 4,4'-bipyridine, HEDP, piperazine and compounds **1** – **4** at room temperature.

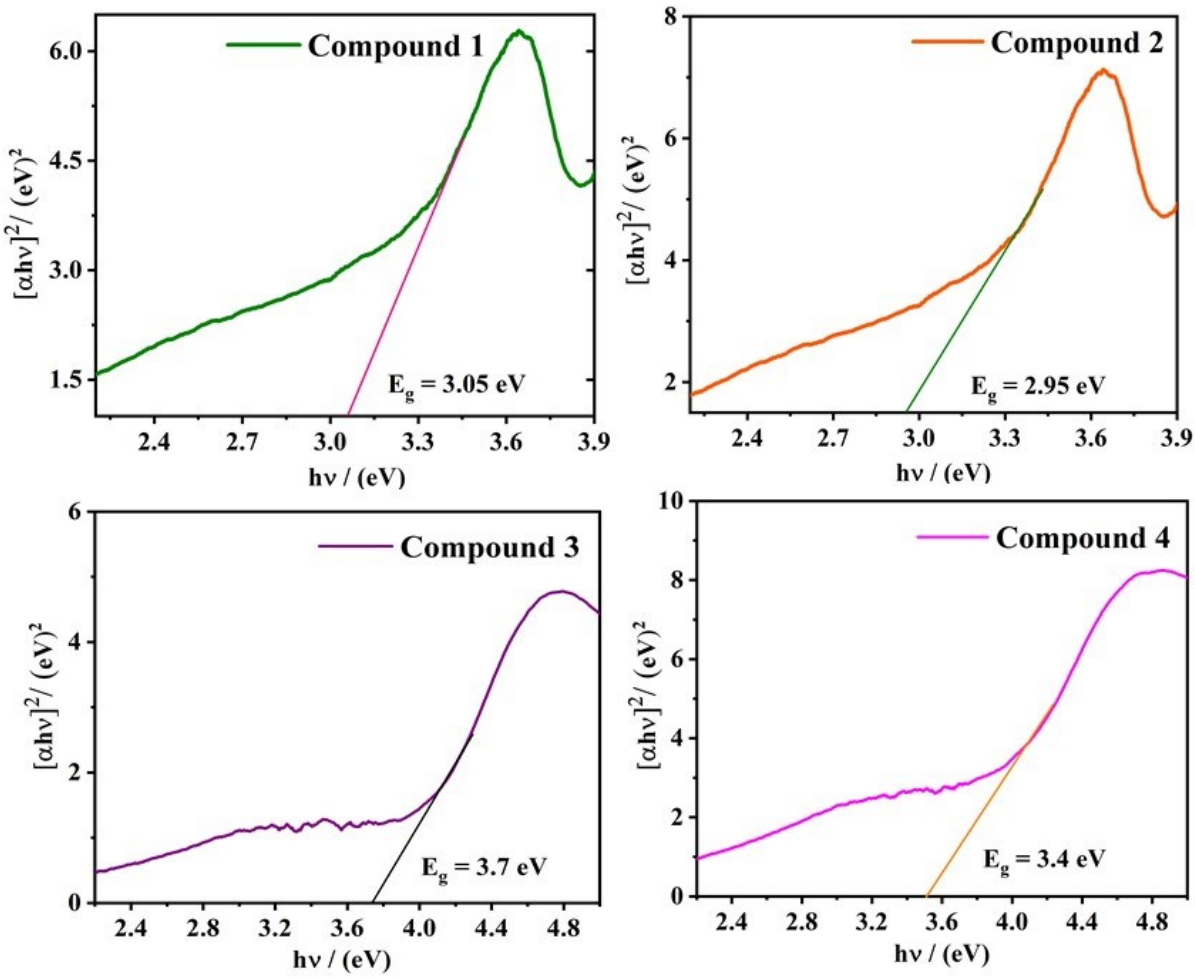

Figure S7: Optical band gap measurement from UV-Visible spectroscopy using Tauc model for Compounds **1** – **4**.

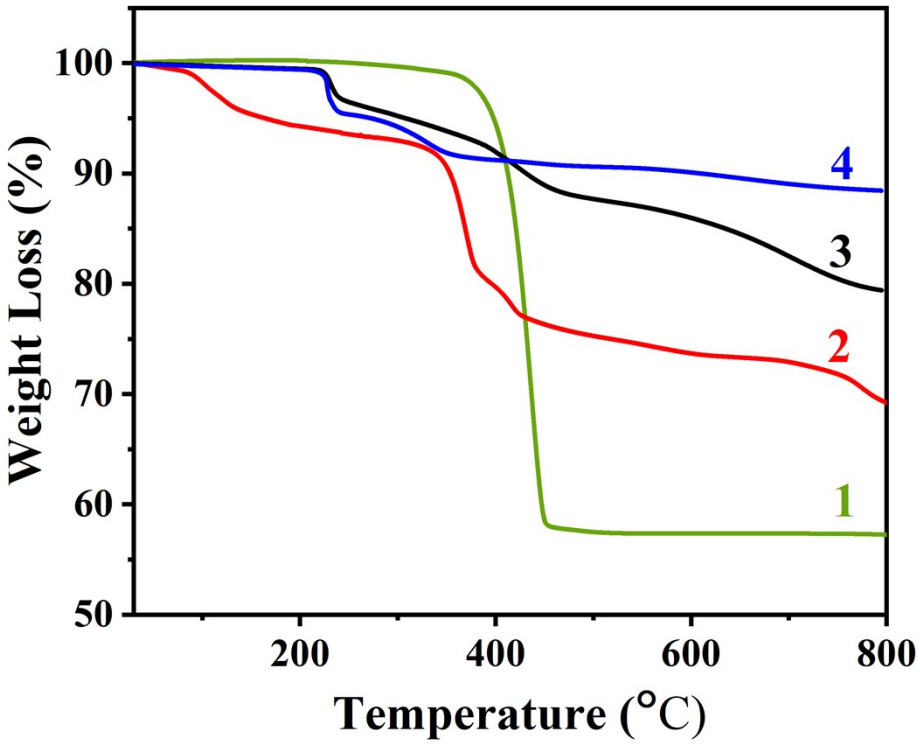

Figure S8: TGA plot for compounds **1 – 4**.

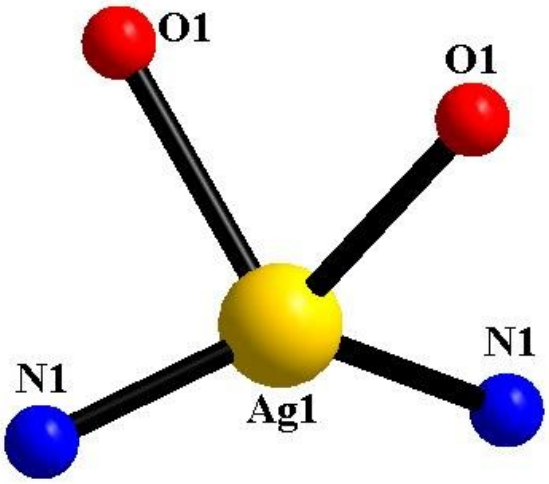

Figure S9: Coordination environment of silver ion (Ag1) for compound **1**.

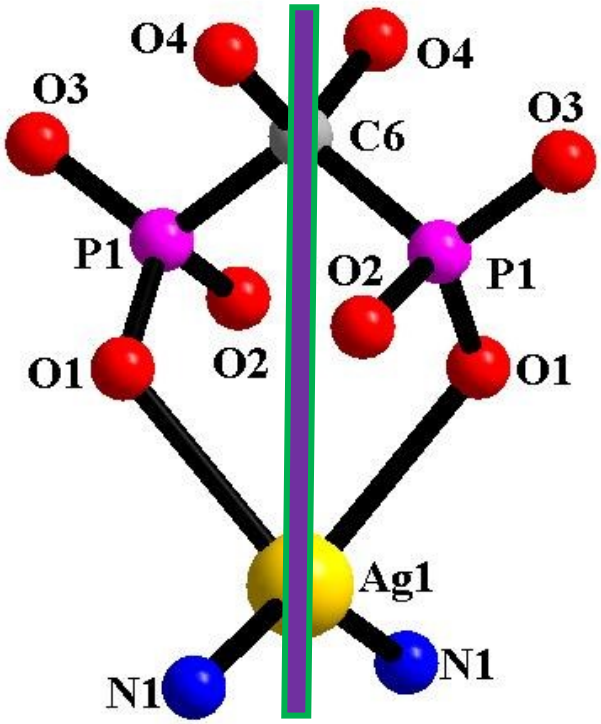

Figure S10: η^2, μ_1 – coordination mode of hedp unit in compound **1.** The structure is drawn by taking *P* 2/*n* space group. The –CH_3 and –OH groups of the diphosphonate ligand were found same in the structure. But the non-centrosymmetric *P n* space group can distinguish two different groups (as given in Figure 1 in the manuscript).

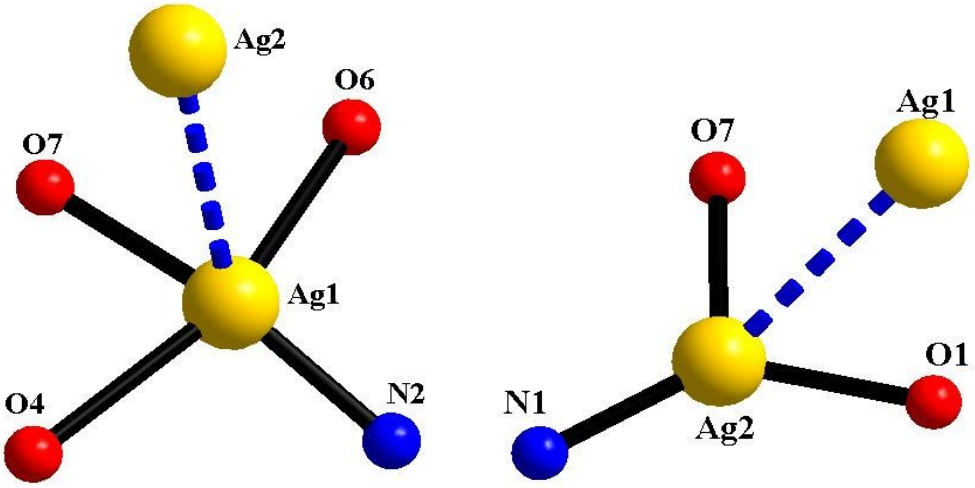

Figure S11: Coordination environment of different silver ions (Ag1 and Ag 2) for compound **2**.

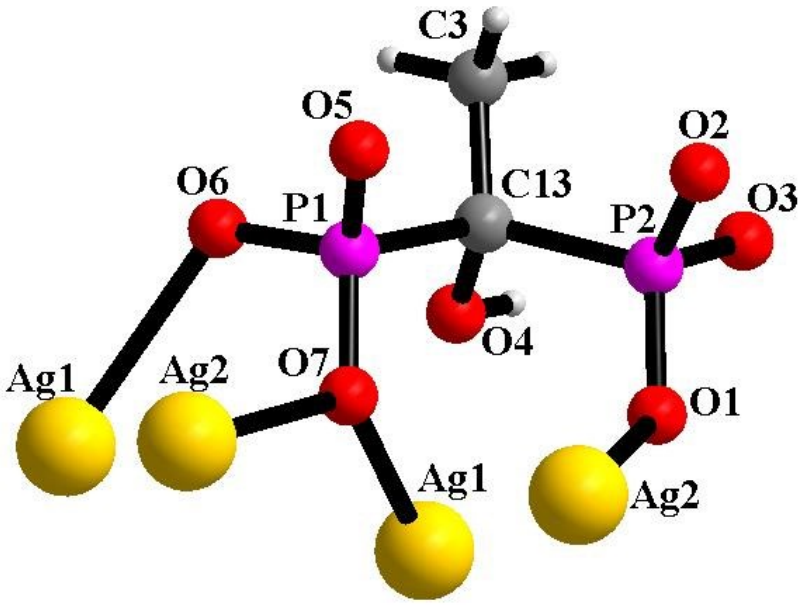

Figure S12: η^2, μ_3 and η^1, μ_1 – coordination mode of hedp unit in compound **2.**

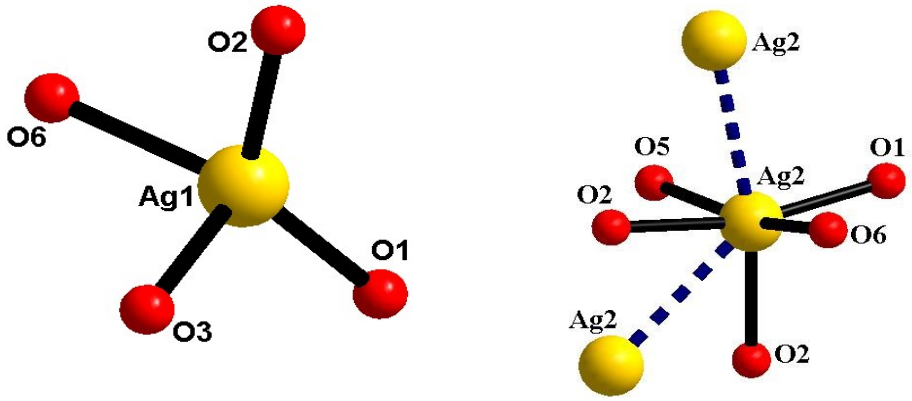

Figure S13: Coordination environment of different silver ions (Ag1 and Ag 2) for compound **3**.

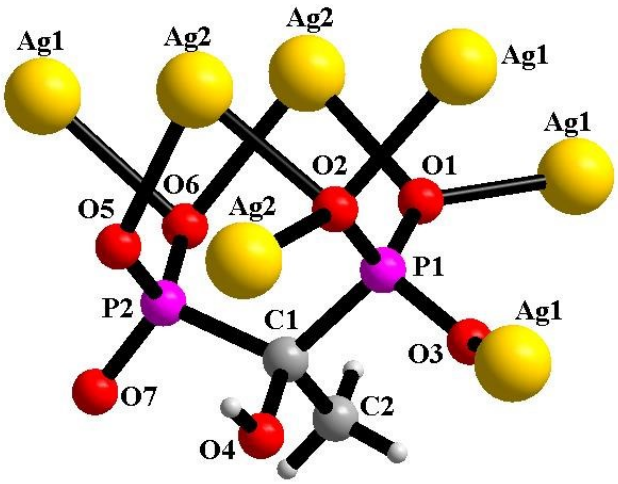

Figure S14: η^3, μ_6 and η^2, μ_3 – coordination mode of hedp unit in compound **3**.

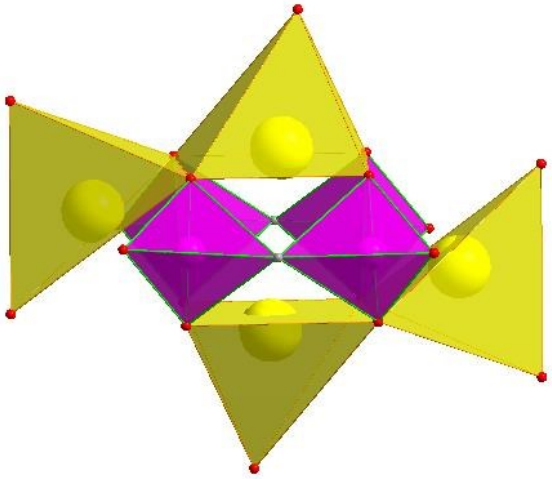

Figure S15: Observed pseudo SBU-8 unit in compound **3**.

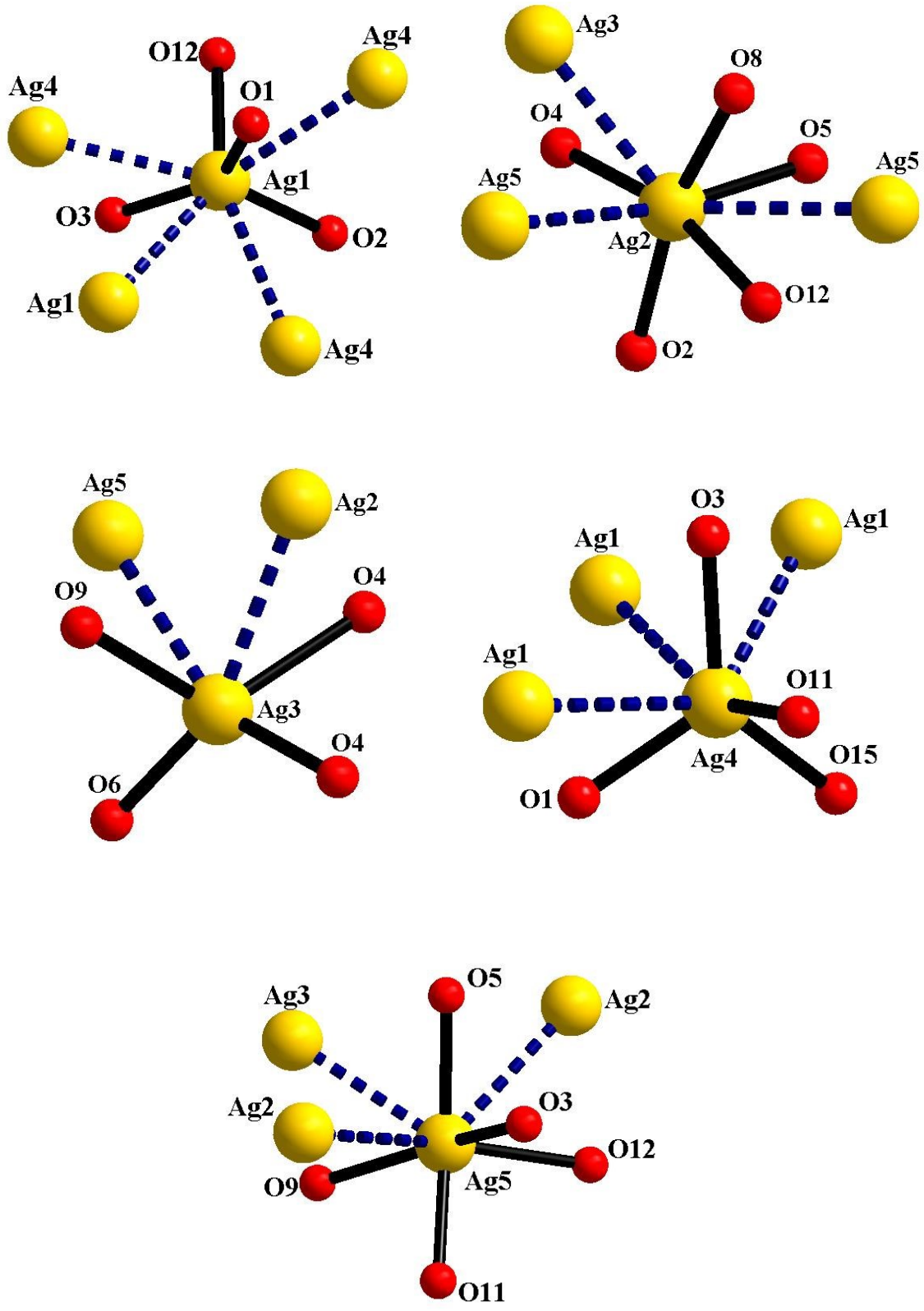

Figure S16: Coordination environment of different silver ions (Ag1 to Ag5) for compound **4**.

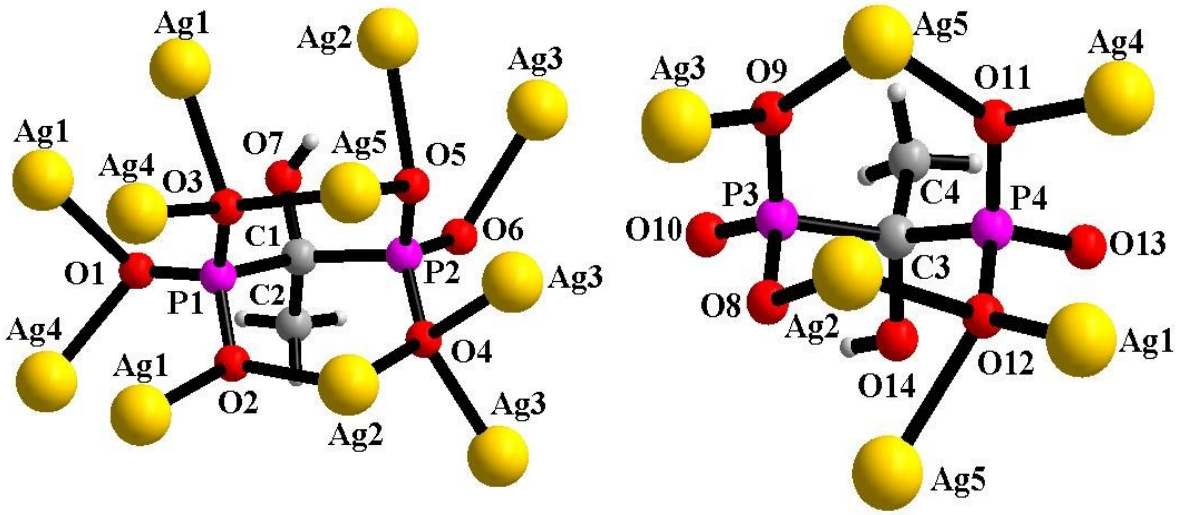

(a) **(b)**

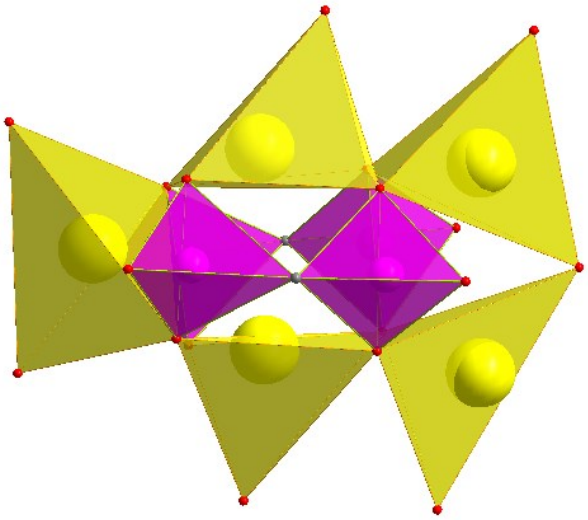

(c)

Figure S17: (a) represent η^3, μ_7 and η^3, μ_6 -coordination modes of hedp(1) unit and **(b)** represent η^2, μ_3 and η^2, μ_5 -coordination modes of hedp(2) unit in compound - **II**. **(c)** Observed pseudo SBU-9 unit in the compound **4**.

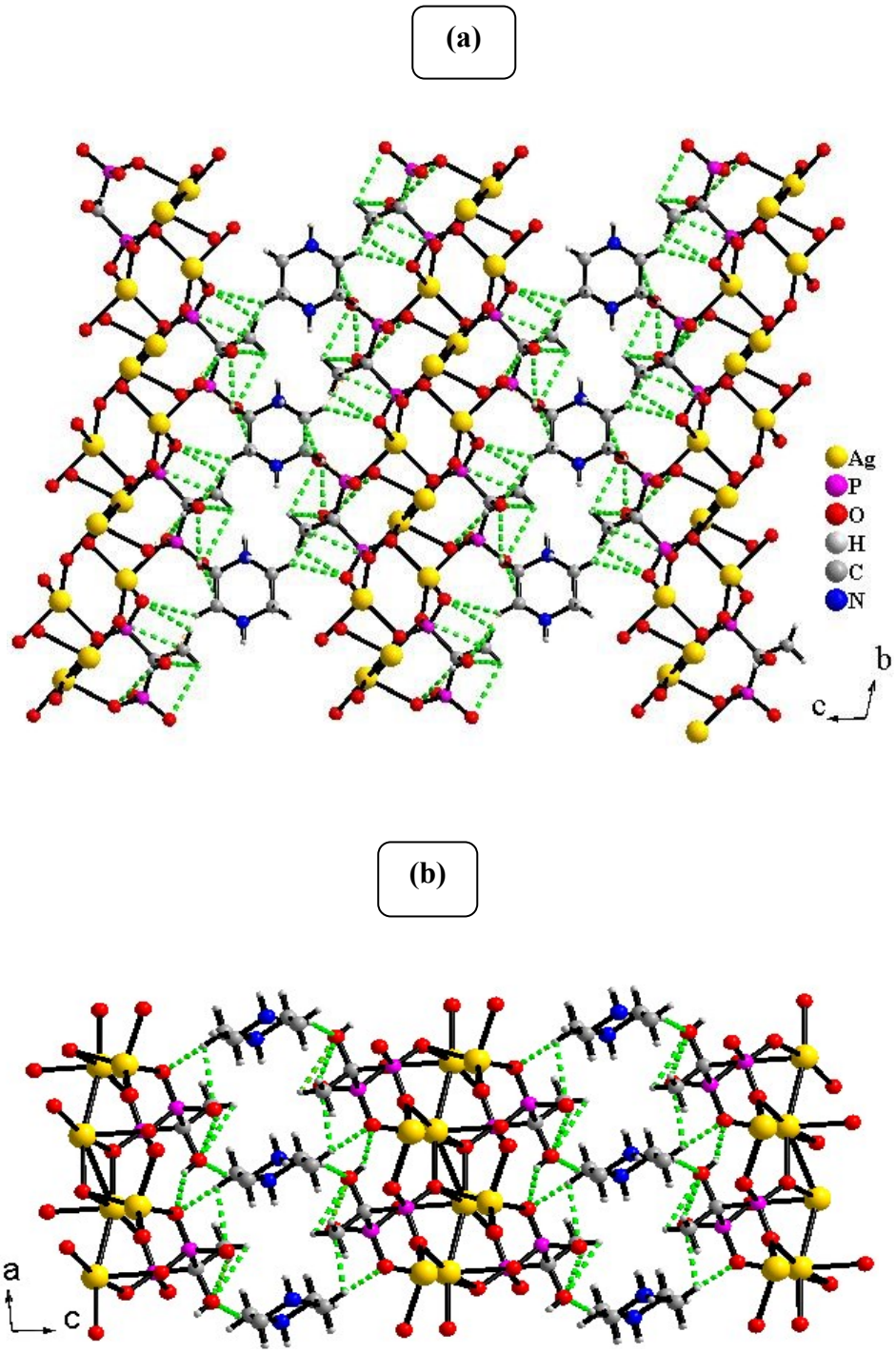

Figure S18: (a) and **(b)** indicates the observed hydrogen bonding interactions in overall 2D packing structure of compounds **3** and **4** respectively.

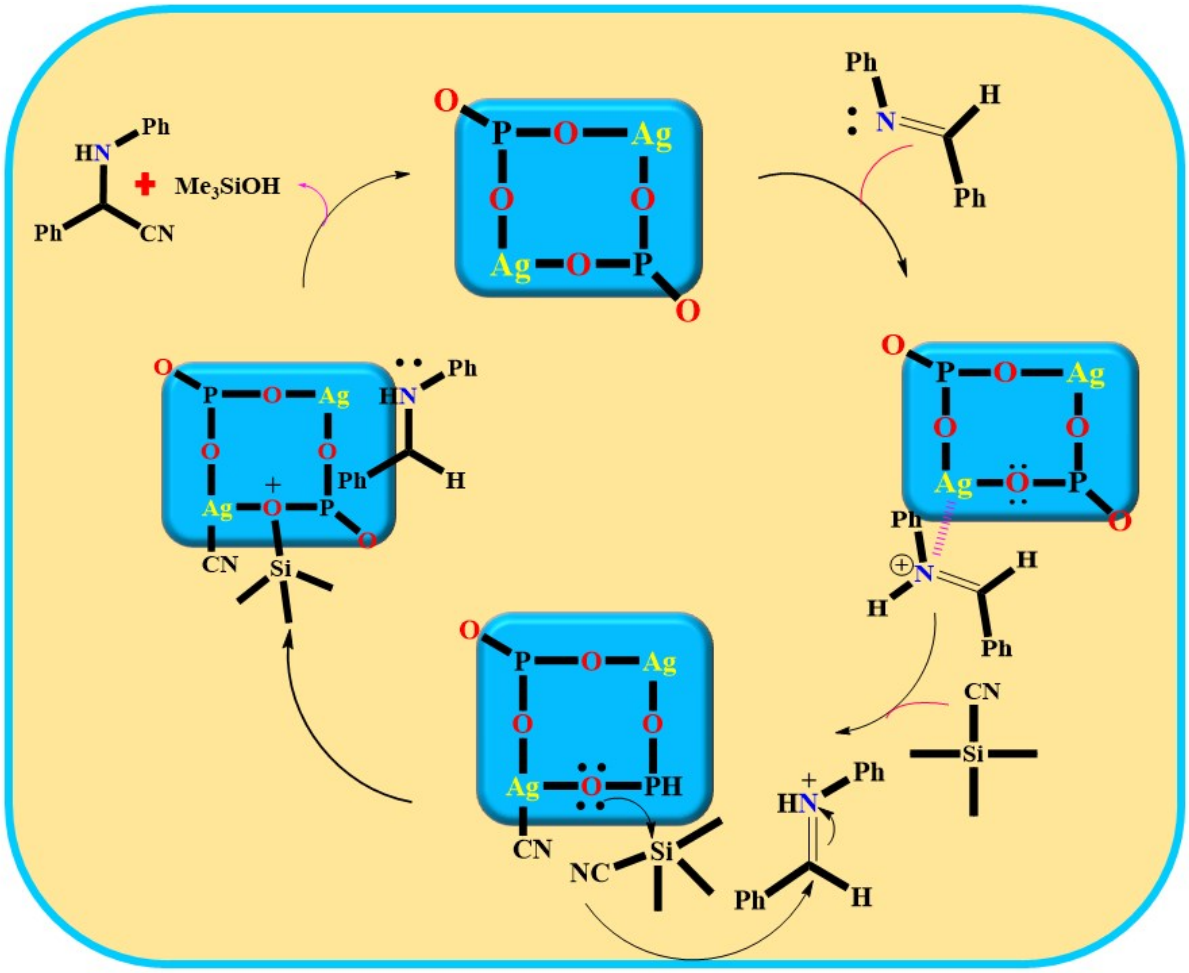

Scheme S1: Proposed mechanism for the Lewis acid catalyzed cyanosilylation of imine.

Here, a weak bond is formed between the lone pair of imine nitrogen and the Lewis acidic silver sites. The oxygen atoms are connected with silver metal ensuring an electron-rich nucleophilic center which facilitates the transfer of electrons to the trimethylsilyl group of TMSCN, resulting in the formation of a weakly coordinated Si−O bond. The terminal water molecule, which may enhance the formation of silicon intermediate, comprises the weaker C−Si bond and enhances the nucleophilicity of cyanide group to form a bond with the Lewis acidic silver surface. Afterward, the nucleophilic −CN group transferred the electrons to carbon and produced cyanosilylated species which eliminate as a product in the next step.

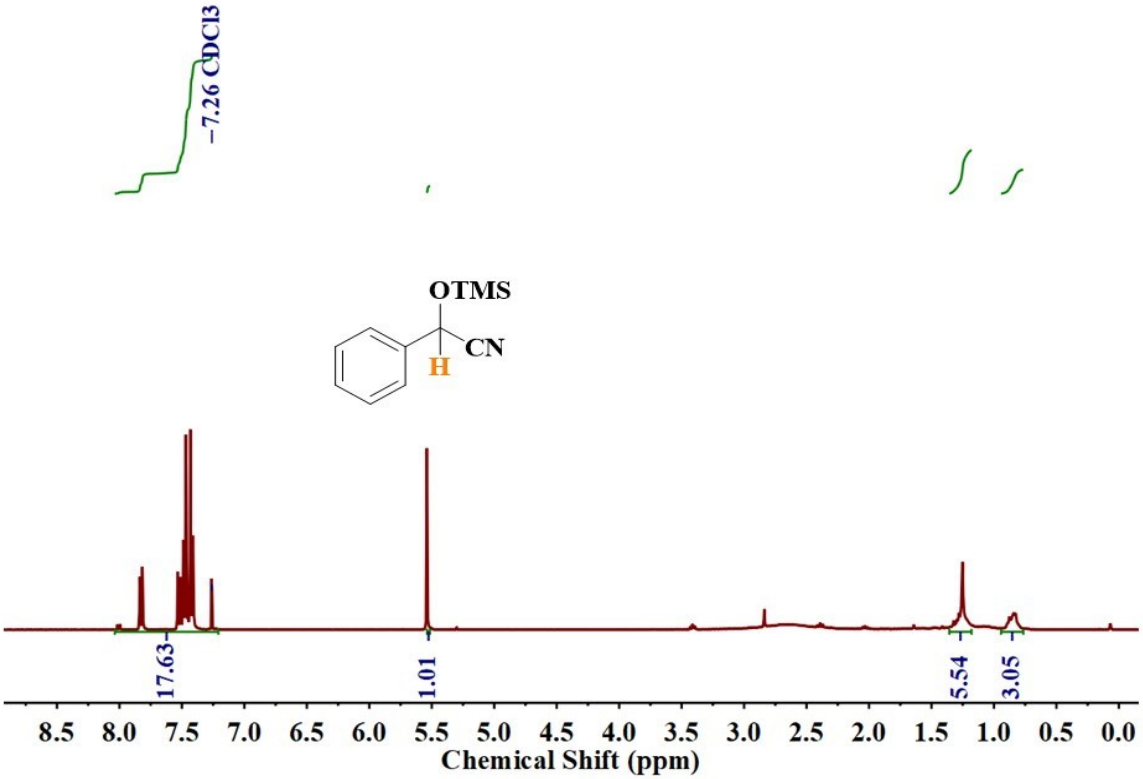

Figure S19: ^{1}H-NMR spectrum corresponding to Table 4, entry 1.

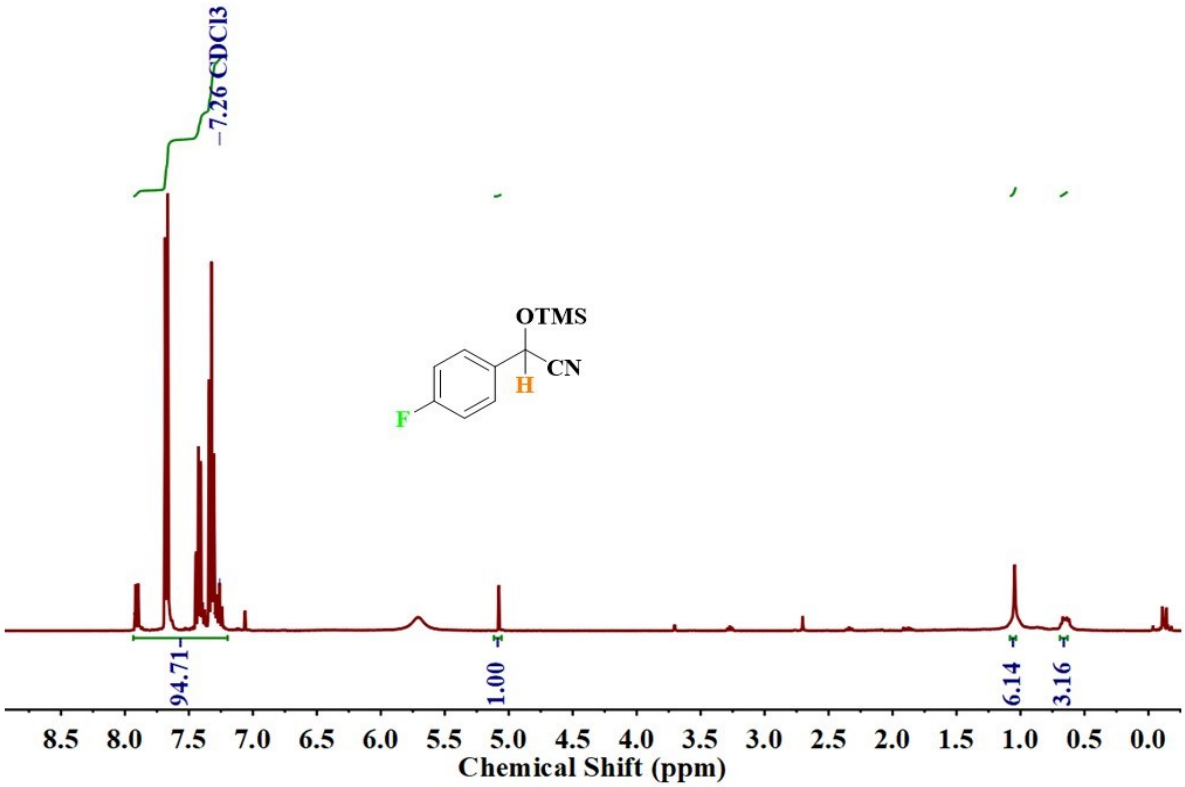

Figure S20: ^{1}H-NMR spectrum corresponding to Table 4, entry 2.

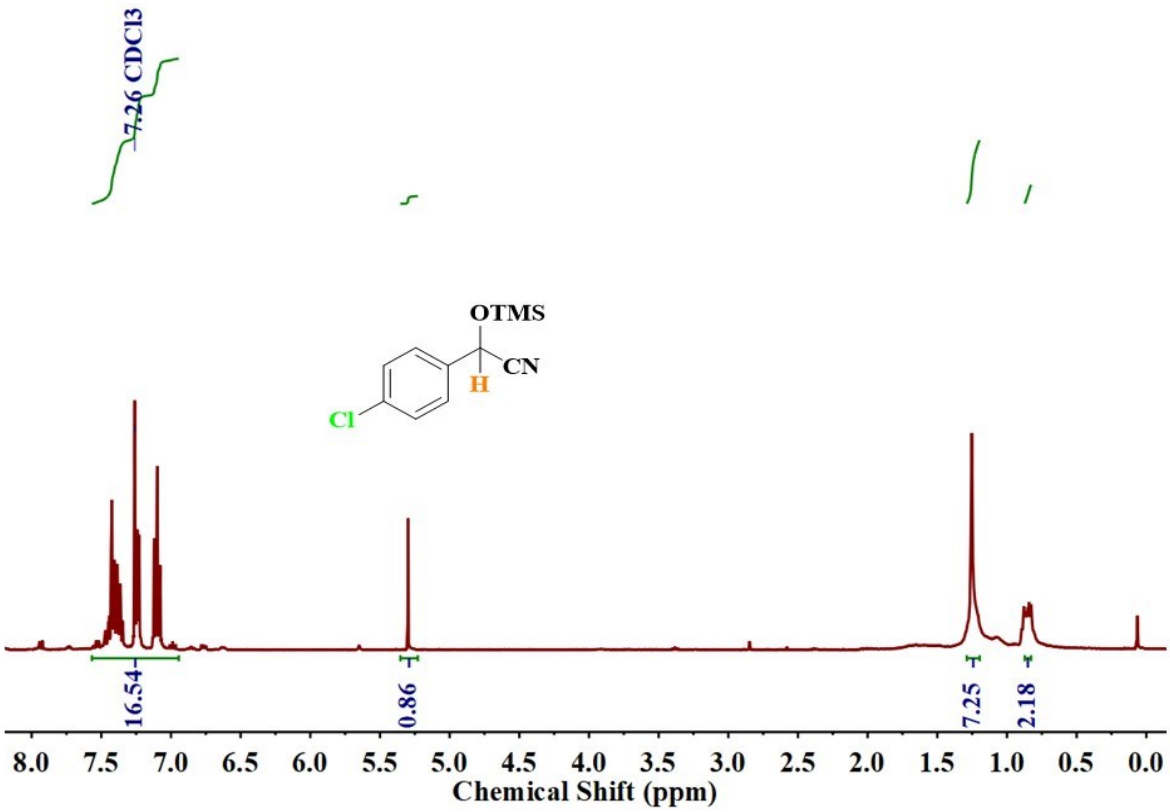

Figure S21: ^{1}H-NMR spectrum corresponding to Table 4, entry 3.

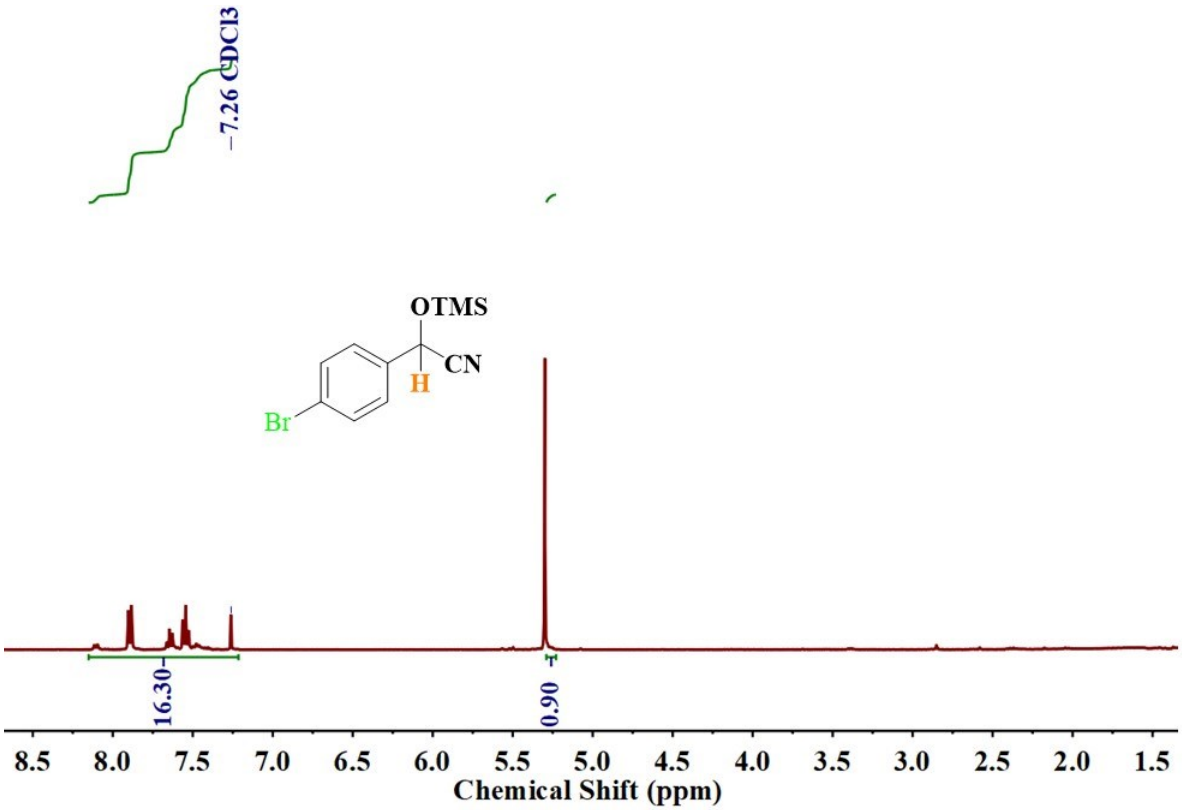

Figure S22: ^{1}H-NMR spectrum corresponding to Table 4, entry 4.

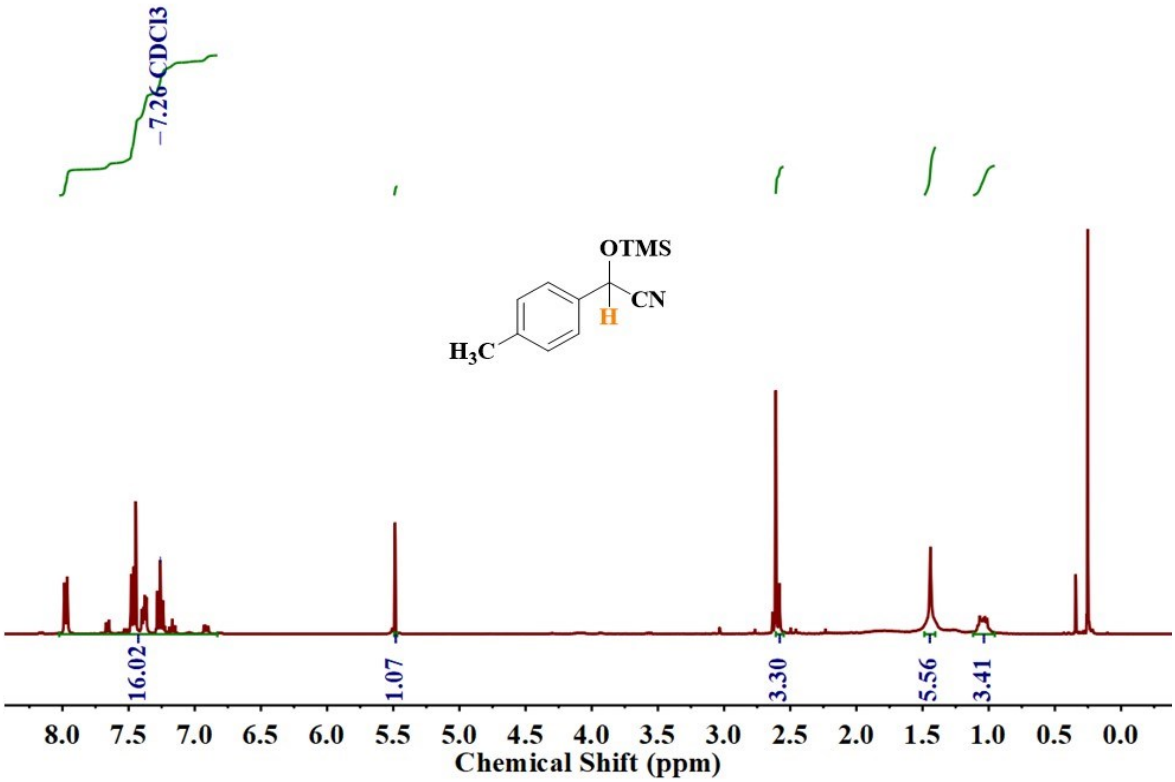

Figure S23: ^{1}H-NMR spectrum corresponding to Table 4, entry 5.

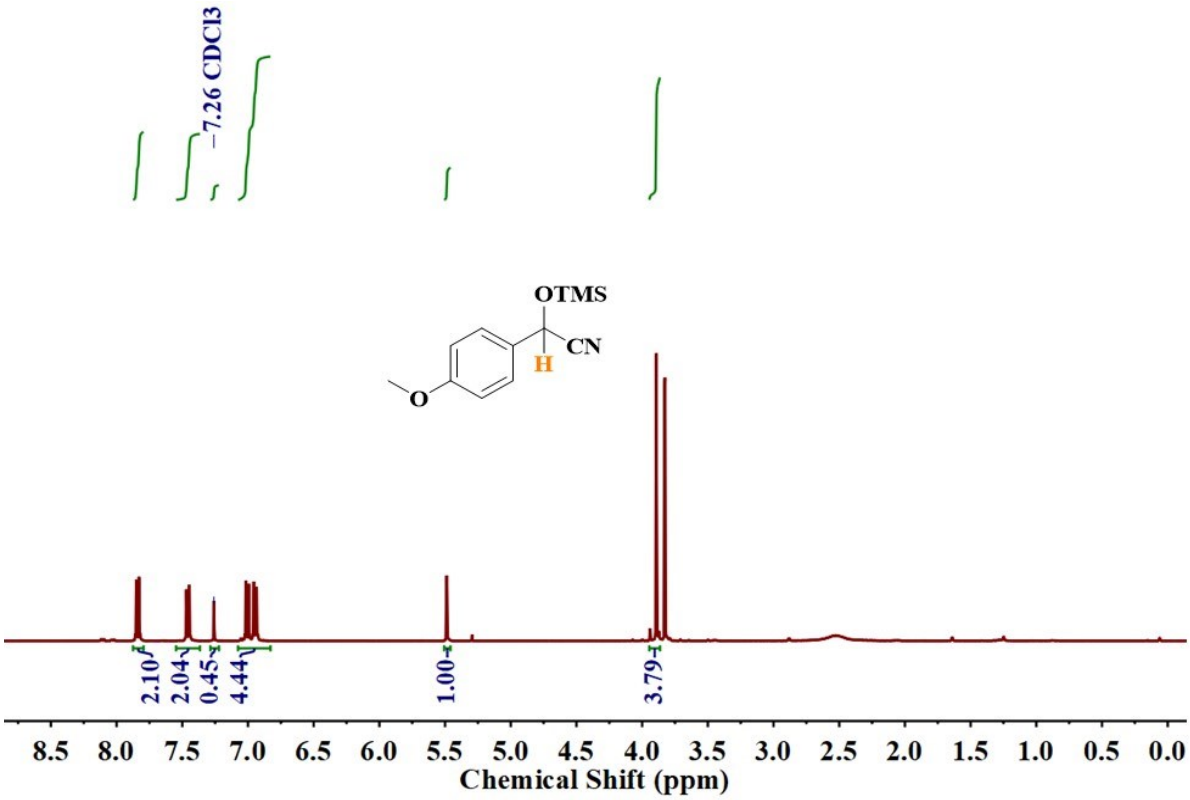

Figure S24: ^{1}H-NMR spectrum corresponding to Table 4, entry 6.

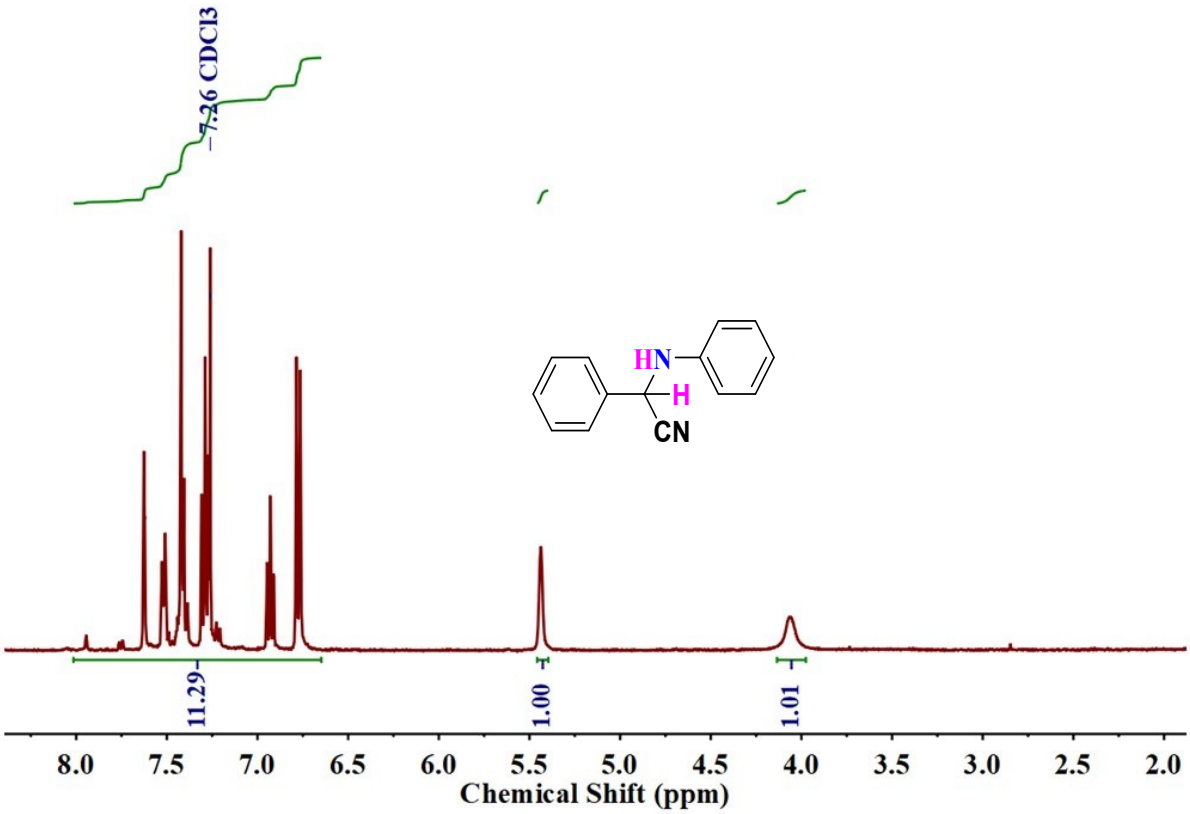

Figure S25: ^{1}H-NMR spectrum corresponding to Table 5, entry 1.

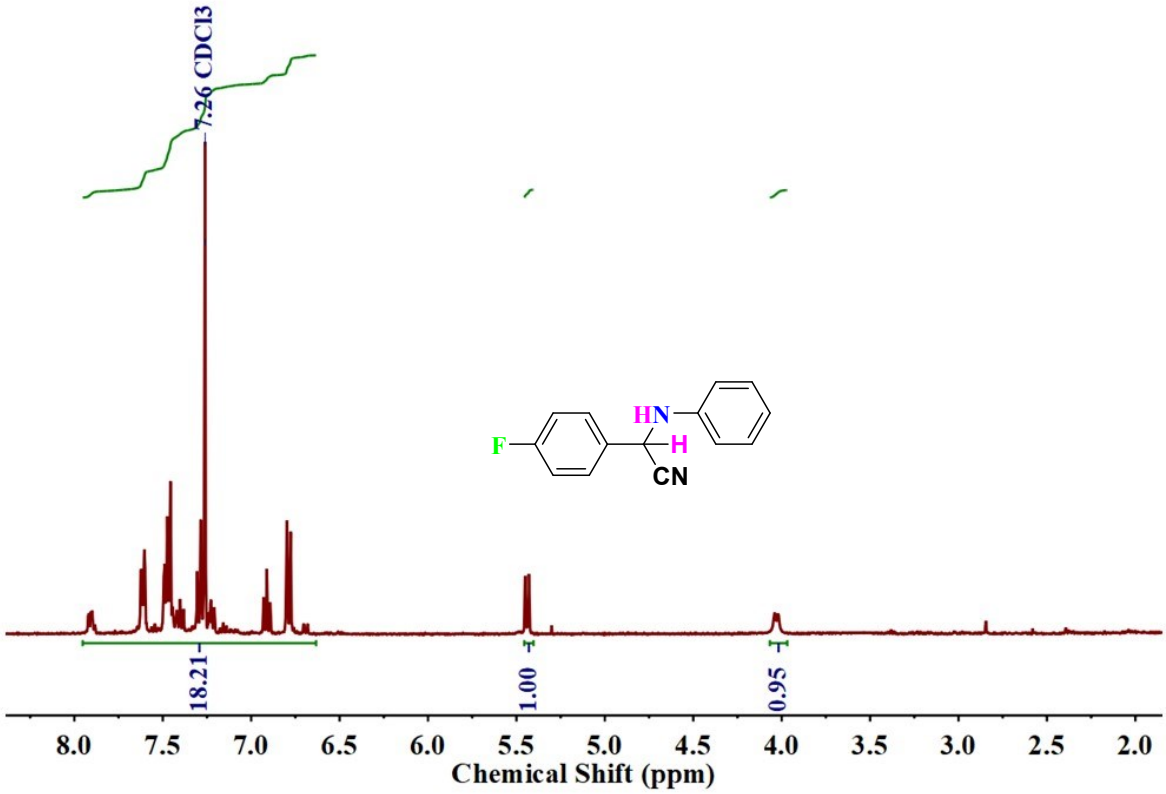

Figure S26: ^{1}H-NMR spectrum corresponding to Table 5, entry 2.

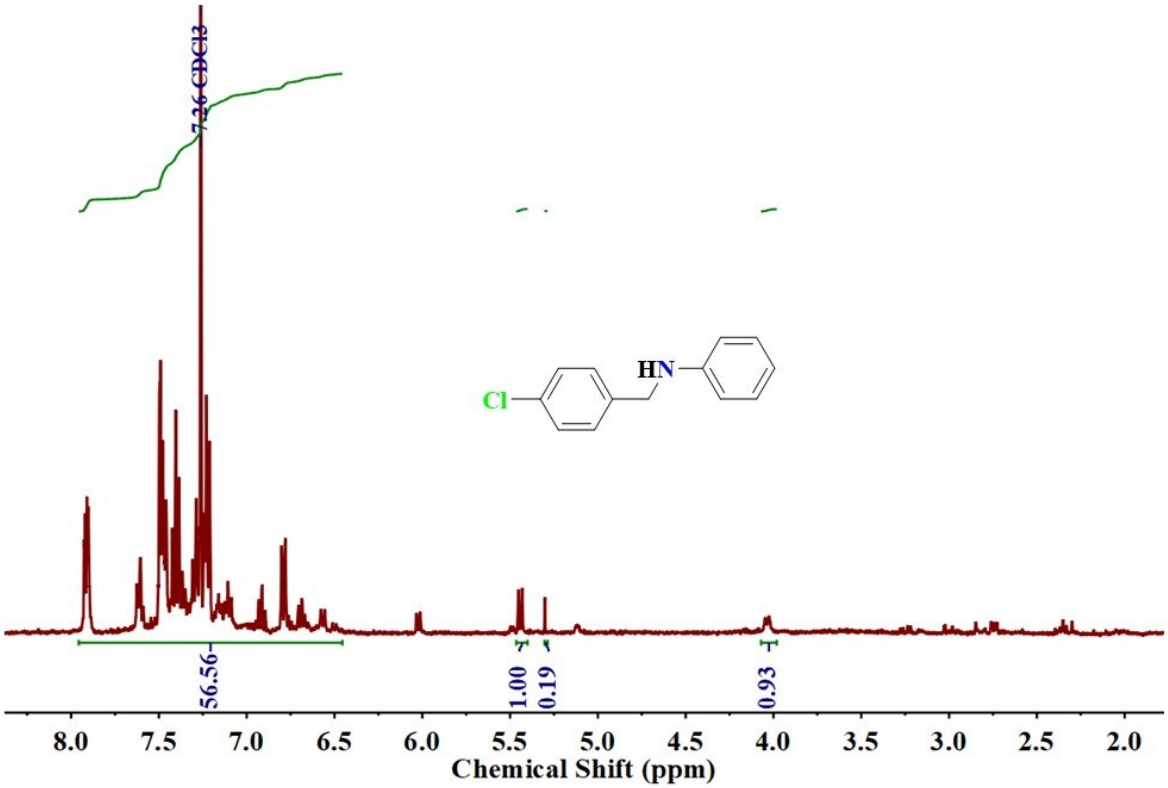

Figure S27: ^{1}H-NMR spectrum corresponding to Table 5, entry 3.

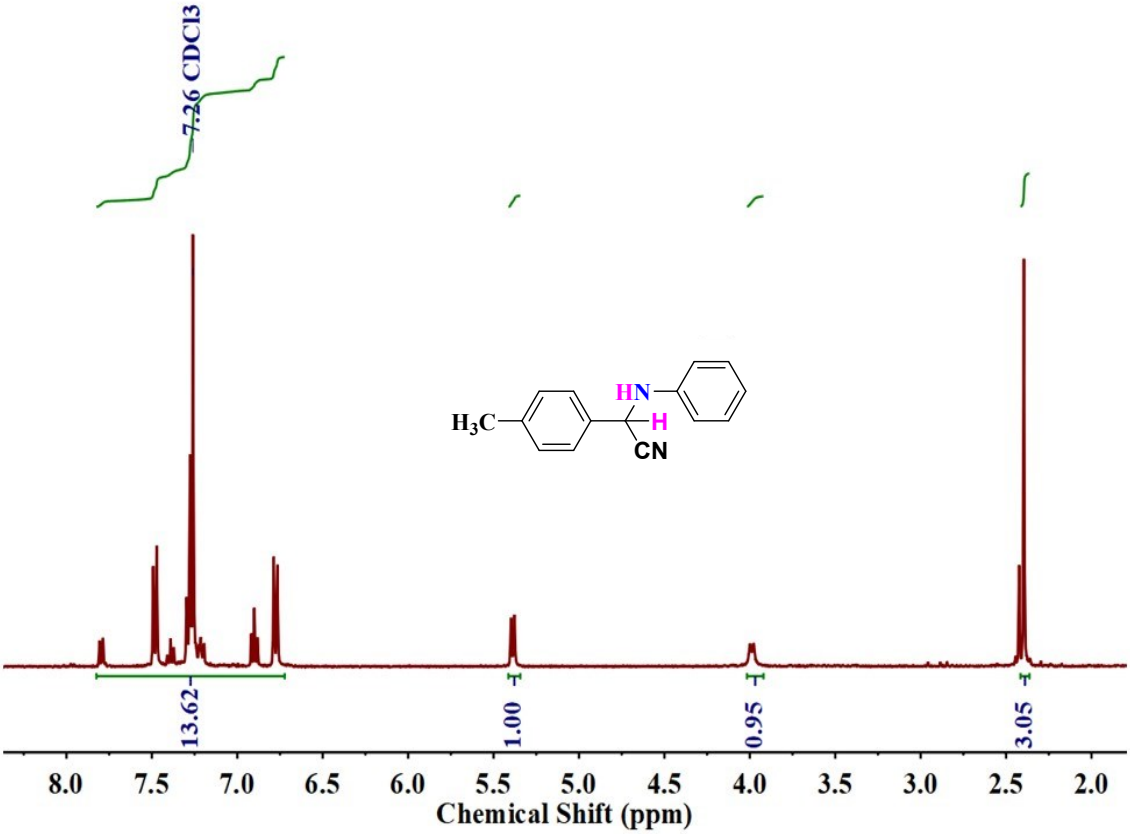

Figure S28: ^{1}H-NMR spectrum corresponding to Table 5, entry 4.

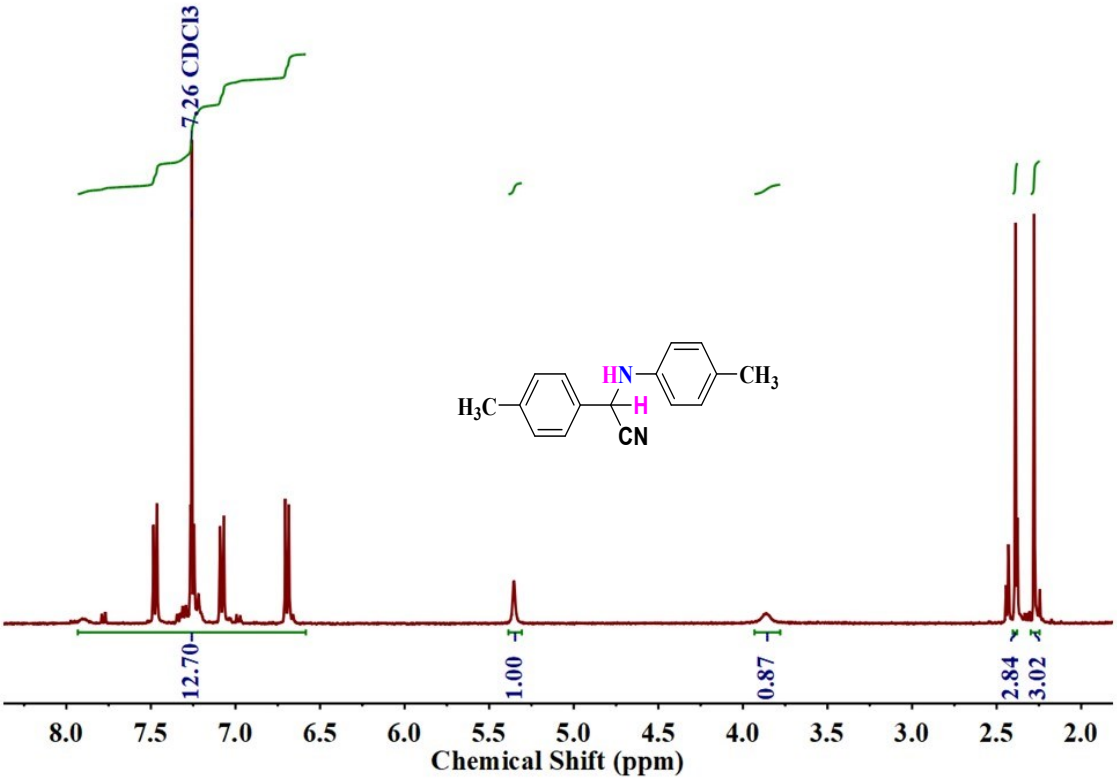

Figure S29: ^{1}H-NMR spectrum corresponding to Table 5, entry 5.

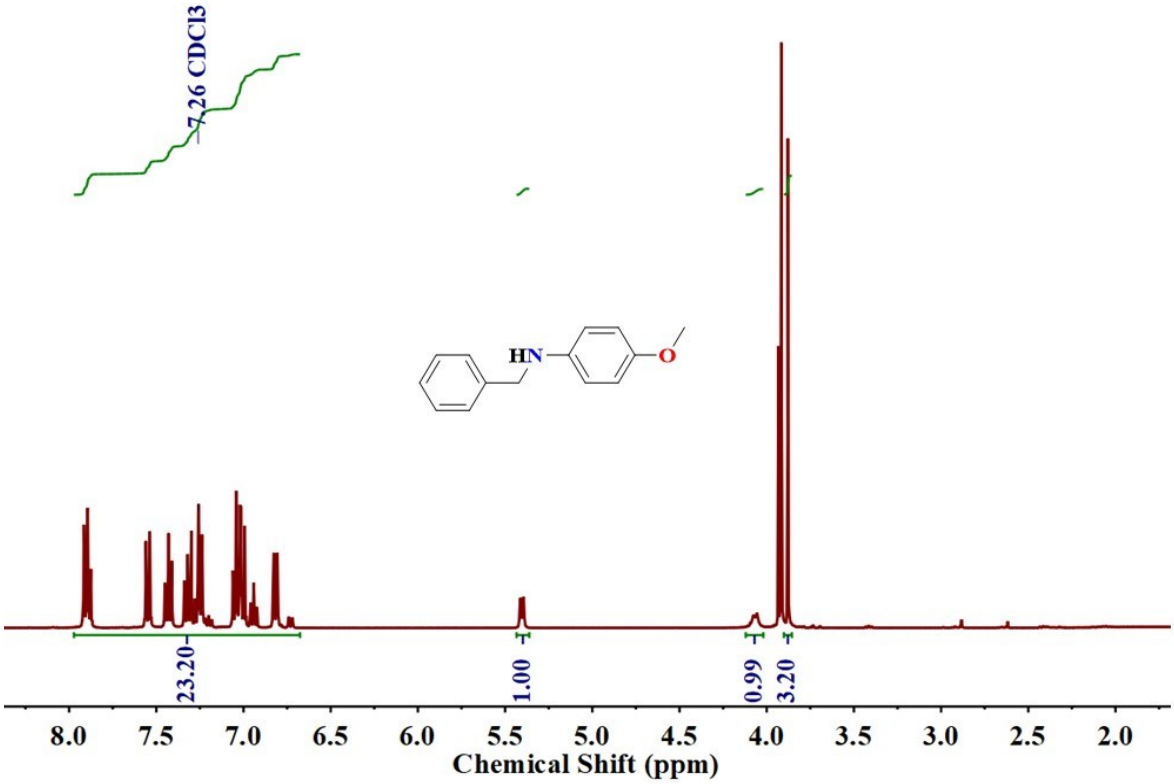

Figure S30: ^{1}H-NMR spectrum corresponding to Table 5, entry 6.

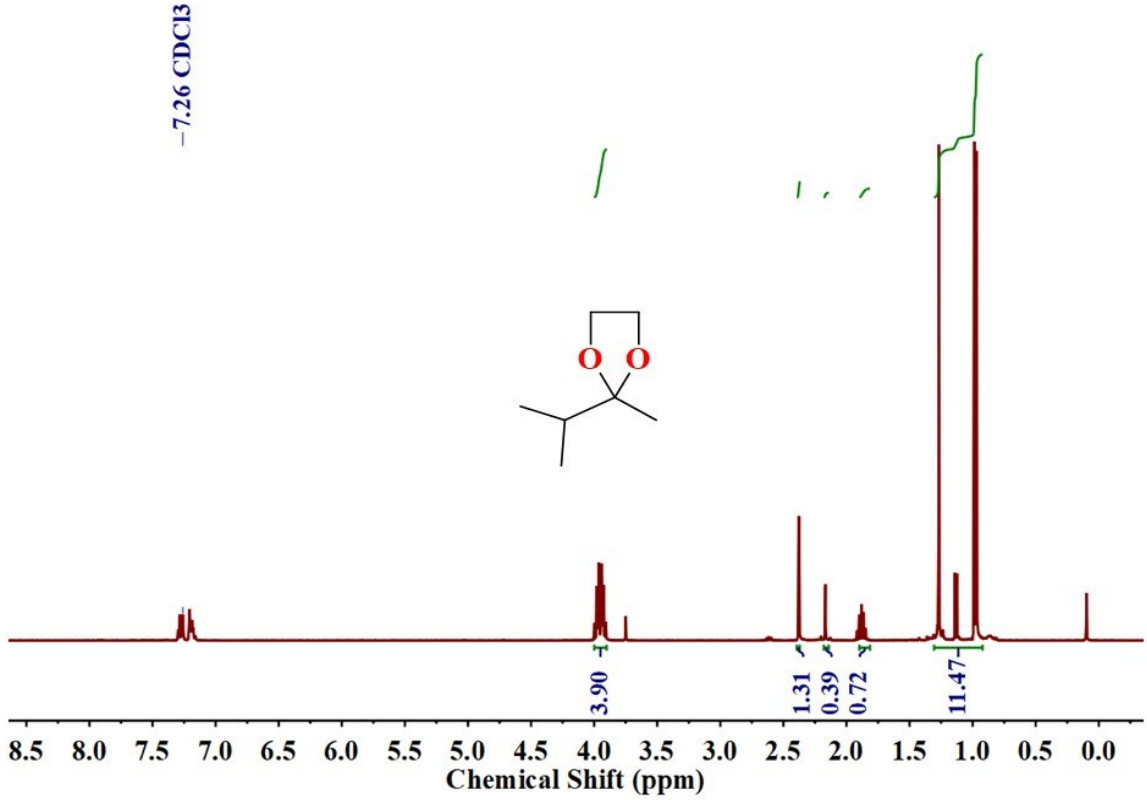

Figure S31: ^{1}H-NMR spectrum of cyclic ketal formation corresponding to Table 6, entry with 3-Methyl-2-butanonae.

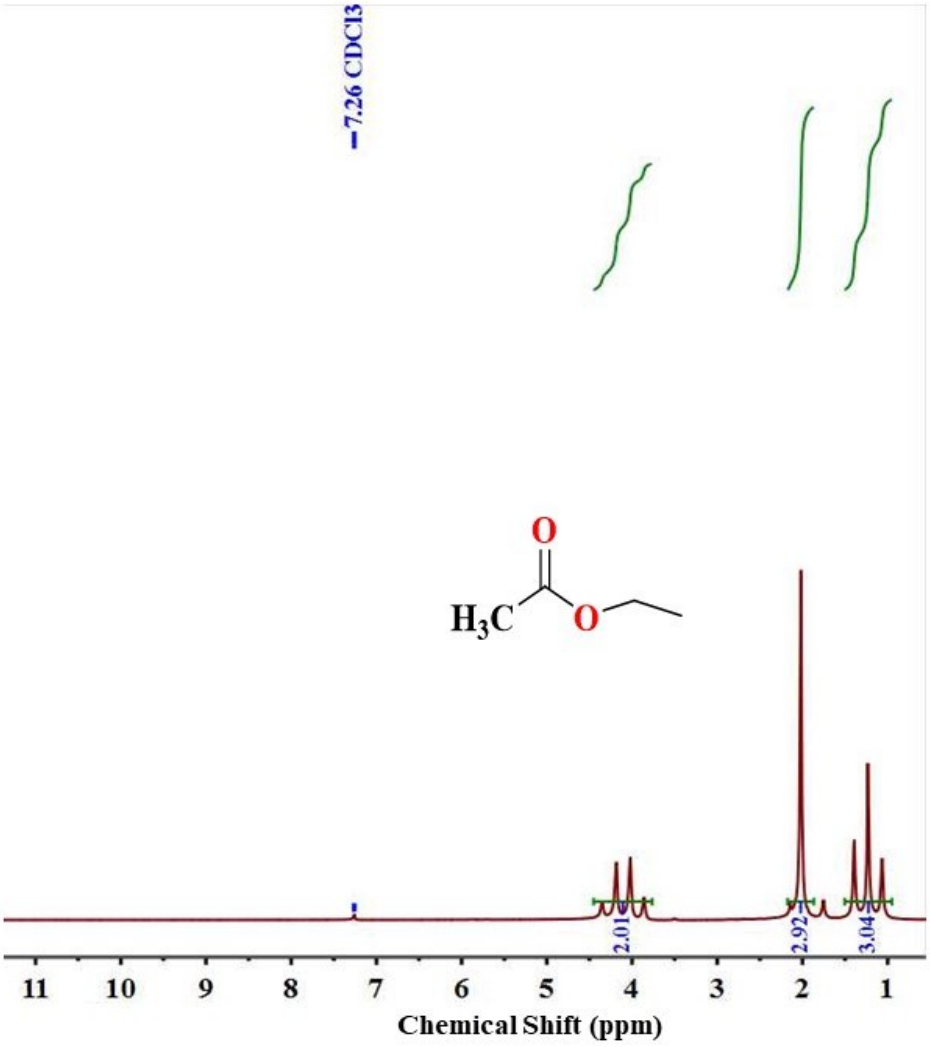

Figure S32: ^{1}H-NMR spectrum of ester formation corresponding to Table 6, entry with acetic acid.

REFERENCES:

1. R. Fu, S. Xia, S. Xiang, S. Hu and X. Wu, Syntheses, characterization and electrical property of a new silver diphosphonate with zeolite-like framework and three-dimensional silver interactions: $[Ag_4(O_3PCH_2CH_2PO_3)]$, *J. Solid State Chem.,* 2004, 4626–4631.
2. A.-G. D. Nelson, Z. Rak, T. E. Albrecht-Schmitt, U. Becker and R. C. Ewing, Three new silver uranyl diphosphonates: structures and properties, *Inorg. Chem.,* 2014, **53**, 2787−2796.
3. X. Hou and S.-F. Tang, Four new silver phosphonates constructed from semi-rigid phosphonate ligands: syntheses, structures and properties, *RSC. Adv.,* 2016, **6**, 100158−100166.
4. Y.-P. Xie and T. C. W. Mak, New synthesis of silver phosphonate complexes from polymeric silver phenylethynide as a structure-directing precursor, *Dalton Trans.,* 2013, **42**, 12869.
5. T. Hu and T. C. W. Mak, Silver(I) multiple salts assembled with phosphonate, perfluorocarboxylate, and the multinuclear silver-ethynediide supramolecular synthon, *Inorg. Chem.,* 2013, **52**, 9066−9076.
6. N. B. Padalwar, B. Akkisetty and K. Vidyasagar, Syntheses and characterization of silver phenylphosphonates and phenylarsonates, $Ag_xH_{4-x}(O_3PPh)_2$ (x = 1–4) and $Ag_xH_{4-x}(O_3AsPh)_2$ (x = 2, 4), *Z. Anorg. Allg. Chem.,* 2014, **640**, 2876–2881.
7. M. Srinu, N. B. Padalwar and K. Vidyasagar, Syntheses and Characterization of 1,4-Phenylenebisphosphonates, $A[HO_3PC_6H_4PO_3H_2]$ (A = Li, K, Rb, Cs, Tl, Ag and NH_4) and Crystal Structure of 1,4-Phenylenebisphosphonic Acid, *Z. Anorg. Allg. Chem.,* 2015, **641**, 2429–2434.
8. Y.-M. Su, H.-F. Su, Z. Wang, Y.-A. Li, S. Schein, Q.-Q. Zhao, X.-P. Wang, C.-H. Tung, D. Sun and L.-S. Zheng, Three silver nests capped by thiolate/phenylphosphonate, *Chem. Eur. J.,* 2018, **24**, 15096–15103.
9. X. Liang, Y. Chen, L. Wang, F. Zhang, Z.-L. Fan, T. Cao, Y. Cao, H. Zhu, X. He, B. Deng, Y. You, Y. Dong and Y. Zhao, E□ect of carbon-skeleton isomerism on the dielectric properties and proton conduction of organic cocrystal compounds assembled from 1,2,4,5-benzenetetracarboxylic acid and piperazine derivatives, *New J. Chem.,* 2019, **43**, 11099.
10. P.-C. Guo, T.-Y. Chen, X.-M. Ren, W.-H. Ning and W. Jin, A low-k dielectric metal–organic-framework compound showing novel three-step dielectric relaxations originating from orientational motion of dipolar guest molecules, *New J. Chem.,* 2014, **38**, 2254.

11. H. Zhang, S.-S. Yu and H.-B. Duan, A hybrid crystal with high dielectric constant and relaxation dielectric behavior, *Inorg. Chem. Commun.,* 2018, **93***,* 1–5.

12. R. Kumari, R. Seera, A. De, R. Ranjan and T. N. Guru Row, Organic multifunctional materials: second harmonic, ferroelectric, and dielectric properties in N-Benzylideneaniline analogues, *Cryst. Growth Des.,* 2019, **19**, 5934−5944.

13. B.-T. Qu, J.-C. Lai, S. Liu, F. Liu, Y.-D. Gao and X.-Z. You, Cu- and Ag-based metal−organic frameworks with 4-pyranone-2,6-dicarboxylic acid: syntheses, crystal structures, and dielectric properties, *Cryst. Growth Des.,* 2015, **15**, 1707−1713.

14. C. Xue, Z.-Y. Yao, S.-X. Liu, H.-B. Luo, Y. Zou, L. Li and X.-M. Ren, dielectric anomaly and relaxation natures in a Zn-Cr pillar−layered metal−organic framework with cages and channels, *J. Solid State Chem.,* 2017, **250**, 107–113.

15. S. Bouketaya, A. Elferjani, M. S. M. Abdelbaky, M. Dammak and S. Garcia-Granda, Crystal structure, phase transitions, dielectric and vibrational studies and photoluminescence properties of a new iron fluoride based on bipyridine, *J. Solid State Chem.,* 2019, **277**, 395–405.

16. H.-X. Zhao, J.-X. Liu, L.-S. Long, A. A. Bokov, Z.-G. Ye, R.-B. Huang and L.-S. Zheng, High dielectric constant and relaxation mechanism of water with hydrated copper(II) ions in a cucurbit[8]uril-based supramolecular architecture, *J. Phys. Chem. C.,* 2012, **116**, 14199−14204.

17. Q.-Z. Shi, Z. Xing, Y.-N. Cao, S.-B. Ma and L.-Z. Chen, Synthesis, structure and dielectric properties of a Cd coordination polymer based on homopiperazine, *J. Mol. Struct.,* 2017, **1130**, 363–367.

18. T.-P. Hu, Y.-Q. Zhao, K. Mei, S.-J. Lin, X.-P. Wang and D. A. Sun, A novel silver(I)-keggin-polyoxometalate inorganic–organic hybrid: a Lewis acid catalyst for cyanosilylation reaction, *CrystEngComm.,* 2015*,* **17**, 5947–5952.

19. S. Li, Y. Zhou, Q. Peng, R. Wang, X. Feng, S. Liu, X. Ma, N. Ma, J. Zhang, Y. Chang, Z. Zheng and X. Chen, Controllable synthesis and catalytic performance of nanocrystals of rare-earth-polyoxometalates, *Inorg. Chem.,* 2018, **57**, 6624–6631.

20. J. M. Moreno, A. Velty, U. Díaz and A. Corma, Synthesis of 2D and 3D MOFs with tuneable Lewis acidity from preformed 1D hybrid sub-domains, *Chem. Sci.,* 2019, **10**, 2053–2066.

21. F.-Z. Jin, C.-C. Zhao, H.-C. Ma, G.-J. Chen and Y.-B. Dong, Homochiral BINAPDA-Zr-MOF for heterogeneous asymmetric cyanosilylation of aldehyde, *Inorg. Chem.* 2019, **58**, 9253−9259.

22. T. Kajiwara, M. Higuchi, A. Yuasa, H. Higashimura and S. Kitagawa, One-dimensional alignment of strong Lewis acid sites in a porous coordination polymer, *Chem. Commun.,* 2013, **49**, 10459–10461.

23. L. Hui, G.-X. Hao, H.-D. Luo, C.-X. Ke, G. Shi, J. Lin, X.-M. Lin, U. Y. Qazi and Y.-P. Cai, Bifunctional 2D Cd(II)-based metal−organic framework as e□cient heterogeneous catalyst for the formation of C−C bond, *Cryst. Growth Des.,* 2018, **18**, 2883−2889.

24. X.-M. Lin, J.-L. Niu, P.-X. Wen, Y. Pang, L. Hu and Y.-P. Cai, A polyhedral metal-organic framework based on the supramolecular building block: catalysis and luminescent sensing of solvent molecules, *Cryst. Growth Des.,* 2016, **16**, 4705−4710.

25. J. Chai, P. Zhang, J. Xu, H. Qi, J. Sun, S. Jing, S. Jing, X. Chen, Y. Fan and L. Wang, An in-based 3D metal-organic framework as heterogeneous Lewis acid catalyst for multi-component Strecker reactions, *Inorganica Chimica Acta*., 2018*,* **479**, 165–171.

26. D. Deng, H. Guo, G. Kang, L. Ma, X. He and B. Ji, In situ generation of functionality in a reactive binicotinic-acid-based ligand for the design of multi-functional copper(II) complexes: syntheses, structures and properties, *CrystEngComm.,* 2015*,* **17**, 1871.

27. O. Ohmori and M. Fujita, Heterogeneous catalysis of a coordination network: cyanosilylation of imines catalyzed by a Cd(II)-(4,4′-bipyridine) square grid complex, *Chem. Commun*., 2004, **1**, 1586–1587.

28. A. K. Paul, U. Sanyal and S. Natarajan, Use of polyazaheterocycles in the assembly of new cadmium sulfate frameworks: synthesis, structure, and properties, *Cryst. Growth Des.,* 2010, **9**, 4161–4175.

29. A. K. Paul, K. Naveen, N. Kumar, R. Kanagaraj, V. M. Vidya and T. Rom, First example of a nonanuclear silver sulfate hybrid cluster: green approach for synthesis of Lewis acid catalyst, *Cryst. Growth Des.,* 2018, **18**, 6411−6416.

30. N. Kumar and A. K. Paul, Triggering Lewis acidic nature through the variation of coordination environment of Cd-Centers in 2D-coordination polymers, *Inorg. Chem.,* 2020, **59**, 1284–1294.

31. A. K. Paul, Synthesis, structure and topological analysis of glycine templated highly stable cadmium sulfate framework: A new Lewis acid catalyst., *J. Mol. Struct.,* 2018, **1157**, 672–678.

32. S. Natarajan and R. Karthik, Interpenetrated and catenated zinc thiosulfates frameworks with dia and qtz nets: synthesis, structure, and properties, *Cryst. Growth Des.,* 2016, **16**, 2239–2248.

33. X. Tan, L. Li, J. Zhang, X. Han, L. Jiang, F. Li and C.-Y. Su, Three-dimensional phosphine metal−organic frameworks assembled from Cu(I) and pyridyl diphosphine, *Chem. Mater.,* 2012*,* **24***,* 480−485.

34. H. Fei, L. Paw U, D. L. Rogow, M. R. Bresler, Y. A. Abdollahian and S. R. J. Oliver, Synthesis, characterization, and catalytic application of a cationic metal-organic framework: Ag_2(4,4´-bipy)$_2$($O_3SCH_2CH_2SO_3$), *Chem. Mater.,* 2010, **22**, 2027–2032.